NASA TECHNICAL MEMORANDUM

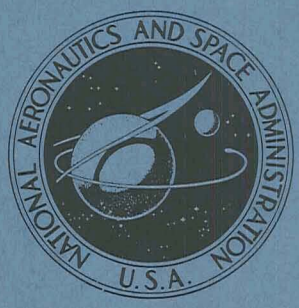

NASA TM X-2368

NASA TM X-2368

SOME FLIGHT-INDUCED ENVIRONMENTAL DATA OBTAINED FROM TWO SIDEWINDER-ARCAS SOUNDING-ROCKET LAUNCHES

by James C. Manning

Langley Research Center
Hampton, Va. 23365

NATIONAL AERONAUTICS AND SPACE ADMINISTRATION • WASHINGTON, D. C. • OCTOBER 1971

1. Report No.	2. Government Accession No.	3. Recipient's Catalog No.
NASA TM X-2368		

4. Title and Subtitle	5. Report Date
SOME FLIGHT-INDUCED ENVIRONMENTAL DATA OBTAINED FROM TWO SIDEWINDER-ARCAS SOUNDING-ROCKET LAUNCHES	October 1971
	6. Performing Organization Code
7. Author(s)	8. Performing Organization Report No.
James C. Manning	L-7869
	10. Work Unit No.
9. Performing Organization Name and Address	607-06-00-01
NASA Langley Research Center Hampton, Va. 23365	11. Contract or Grant No.
	13. Type of Report and Period Covered
12. Sponsoring Agency Name and Address	Technical Memorandum
National Aeronautics and Space Administration Washington, D.C. 20546	14. Sponsoring Agency Code

15. Supplementary Notes

16. Abstract

Some flight-induced environmental data from two Sidewinder-Arcas sounding rockets launched at the White Sands Missile Range are presented. The data obtained were acceleration, structural vibration, internal temperature, heating rate, and roll rate. The measured flight structural data indicate that the vibrations occurring after the rocket ignition shock have amplitudes less than 1.5g along the longitudinal axis and less than 0.6g along the normal axis and that the maximum quasi-static acceleration is about 32g along the longitudinal axis (1g = 9.8 m/sec^2). The measured thermal data indicate that the maximum payload internal temperature is 44.4° C (112° F) and the maximum heat rate is 38 kW/m^2 (3.35 Btu/ft^2-sec). The second stage reached a maximum roll rate of 4.3 cps at second-stage burnout.

17. Key Words (Suggested by Author(s))	18. Distribution Statement
Sounding rocket Meteorological rocket	Unclassified – Unlimited

19. Security Classif. (of this report)	20. Security Classif. (of this page)	21. No. of Pages	22. Price*
Unclassified	Unclassified	38	$3.00

*For sale by the National Technical Information Service, Springfield, Virginia 22151

SOME FLIGHT-INDUCED ENVIRONMENTAL DATA OBTAINED FROM TWO SIDEWINDER-ARCAS SOUNDING-ROCKET LAUNCHES

By James C. Manning
Langley Research Center

SUMMARY

Some flight-induced environmental data from two Sidewinder-Arcas sounding rockets launched at the White Sands Missile Range are presented. The data obtained were acceleration, structural vibration, internal temperature, heating rate, and roll rate. The measured flight structural data indicate that the vibrations occurring after the rocket ignition shock have amplitudes less than 1.5g along the longitudinal axis and less than 0.6g along the normal axis and that the maximum quasi-static acceleration is about 32g along the longitudinal axis ($1g = 9.8\ m/sec^2$). The measured thermal data indicate that the maximum payload internal temperature is 44.4° C (112° F) and that the maximum heat rate is 38 kW/m^2 (3.35 Btu/ft^2-sec). The second stage reached a maximum roll rate of 4.3 cps at second-stage burnout.

INTRODUCTION

Small meteorological sounding-rocket systems have been proven as a valuable tool for atmospheric research in the altitude region extending from about 30 km (98 000 ft) to about 65 km (213 000 ft). To increase the effectiveness of the rocket probings in and above this region of the atmosphere, programs are under way to develop reliable and economical meteorological sounding-rocket systems. One of the important phases of such programs is the flight testing of relatively inexpensive sensors for measuring the basic meteorological parameters above 60 km (197 000 ft). Many flight tests are required during the sensor development to determine the operational characteristics (such as transmitter frequency stability during both ascent and descent) and the reliability of new components, to determine the accuracy and repeatability of the measurements of meteorological data, and to establish the usefulness of the payloads in field-measurements programs. An economical launch-vehicle system is an essential requirement for such flight testing of new sensor concepts.

The Sidewinder-Arcas rocket system is a promising economical tool for obtaining the altitude required for flight testing. Therefore, two Sidewinder-Arcas rocket systems were launched from the White Sands Small Missile Range on June 24 and June 29, 1970,

for vehicle qualification and certification. Since little flight-induced environmental data for the Sidewinder-Arcas rocket system are available, quasi-static and dynamic launch and in-flight loads were measured in these flights and recorded by onboard miniature magnetic tape recorders. These data are required for establishing accurate environmental levels to design and test future sensor systems for flight on this vehicle system. This paper presents the results of these flight tests.

Measurements and calculations were made in the U.S. Customary Units. They are presented herein in the International System of Units (SI) with equivalent values given parenthetically in U.S. Customary Units.

VEHICLE DESCRIPTION

The Sidewinder-Arcas vehicle, figures 1 and 2, is a two-stage, solid-propellant, unguided, sounding rocket stabilized by four fins in a cruciform configuration on each stage. The stages are mated by a bayonet-type interstage transition section that is securely attached to the first stage and slip-fits into the adapter of the second stage. Separation is achieved at burnout of the first stage by differential drag forces. Ignition of the second stage is delayed for about $2\frac{1}{2}$ seconds after burnout of the first stage. The sequence of these and other events is shown in figure 3. The system weights are shown in table I for the sequence illustrated in the mission profile.

The first stage is a Sidewinder Mk 17 Mod 1 rocket motor that was developed by the Department of Defense as an air-to-air missile. It is fitted with the straight Sidewinder fins and an interstage transition section that includes the head end closure for the booster. The Sidewinder motor has an internal burning grain with a normal burn time of approximately 2.4 seconds. As illustrated in figure 2, the booster is 12.7 cm (5.0 in.) in diameter and 190.2 cm (74.9 in.) long.

The second stage is a MARC 2C2 HV-Arcas sounding rocket powered by an end-burning, plastisol-type, solid-propellant grain, generating an average thrust level of about 1468 N (330 lb) with a nominal burn time of 30 seconds. A pyrotechnic 5-second-delay squib in the igniter is electrically actuated at launch; thus, Arcas ignition occurs at approximately 5 seconds after lift-off. The Arcas fins are solid aluminum with steel caps on the leading edges for protection from aerodynamic heating. Each fin is canted at $0^{o}12'$, which induces a roll rate of approximately 4 cycles per second at Arcas burnout.

The payload gas-generating separation device is an integral part of the Arcas rocket head end closure and has a pyrotechnic delay of about 140 seconds. Since the pyrotechnic delay was ignited as the combustion of the Arcas motor grain neared completion (about 35 sec after lift-off), payload separation occurred at about 175 seconds, figure 3.

PAYLOAD DESCRIPTION

The payload configuration used during the flight tests is shown in figure 4. Some of the physical characteristics and instrumentation contained in the payloads are listed in table II. Because of internal space limitations, two payloads were necessary to measure the desired parameters. The parameters measured by payload 1 were acceleration, heat rate, and internal temperature; and those measured by payload 2 were acceleration, roll rate, and structural vibration. Both payloads utilized wideband FM techniques of recording data on magnetic tape. An onboard timing system was included to aid in accurately correlating the measured flight-induced environmental data with ground-based radar tracking and cinetheodolite data. To correct data distortion due to wow (low-frequency flutter) and flutter-speed variations in the onboard-type recorder system, a compensation signal of 25 kHz was recorded on one channel during the data period. This signal was used by ground playback equipment during data reduction to compensate for speed variations.

External power to the payload was provided through the power-control subsystem. This subsystem consisted of relays and logic circuitry either to provide external power to the payloads or to place the payloads on internal battery power. Each payload had two monitors, tape-run and current. The tape-run monitor utilized a prerecorded signal on one channel to provide a positive indication that the tape recorder was running prior to lift-off. The current monitor, which consisted of a 0.1-ohm power resistor in series with the return line of the payload, provided an indication of the total current through the payload prior to lift-off.

Both payloads were equipped with an onboard CW recovery beacon to aid in the location of the payloads. The beacon was a Microcom model XB10-NL operating on a frequency of 235 MHz with an output of 200 mW.

Instrumentation block diagrams of payloads 1 and 2 are shown in figures 5 and 6, respectively. Wideband FM technique of magnetic tape recording is used in order to obtain high-frequency measurements that are extremely desirable in measurements of vibration. In this technique the transducer output signal is fed into a voltage-control oscillator (VCO); therefore, the operating frequency of the VCO is a function of the transducer output signal. The VCO output signal is then recorded on magnetic tape. The tape recorder is operated at a speed of 38 cm/sec (15 in./sec) permitting a frequency response of 100 to 25 000 Hz within ±3 dB. However, the overall-system response is limited to 2.5 kHz within ±3 dB because of the VCO response.

The locations of the transducers of payloads 1 and 2 are shown in figures 7 and 8, respectively.

A disk-gap-band meteorological parachute 5.06 m (16.6 ft) in diameter was used in the recovery of the payload. (See fig. 9.) The parachute utilizes a water-vapor pressurized torus as an inflation aid to assist in opening the canopy at low dynamic pressures.

DISCUSSION OF RESULTS

The onboard environmental-data period terminated at about 80 seconds after lift-off (see fig. 3) because the tape supply was expended. Altitude and velocity data of the test vehicle were obtained by velocimeter and cinetheodolite from lift-off until about 10 seconds and by FPS-16 radar from acquisition, about 27 seconds, to payload separation. These data are shown in figures 10 and 11.

Time Histories

Time histories of altitude for both flight tests are shown in figure 10. Apogees obtained were about 96 km (314 000 ft) and 104 km (340 000 ft) for flights 1 and 2, respectively. The large difference in apogee is due in part to an abrupt change in the low-level wind profile during the launch of flight 1 which caused a lower effective launch angle than anticipated. Time histories of vehicle velocity for both flights are shown in figure 11. As can be seen from the curves, the velocity data for both flights are quite similar with the exception of the velocity at apogee. It is believed that the higher velocity of flight 1 near apogee is caused partially by the somewhat flatter trajectory obtained in that flight.

Figure 12 presents the dynamic-pressure history derived for the first 70 seconds of each flight. The time histories are computed from the measured velocity and the density for 30° north latitude for July from reference 1. The maximum dynamic pressure occurred at Sidewinder burnout or at approximately 2.4 seconds.

Internal Temperature

The payload internal temperature on the launch pad was a function of ambient temperature, sun exposure, and heat output of the payload electronics. After launch, the internal temperature was a function of the compartment temperature prior to launch, vehicle flight path, duration of flight, heat output of the payload electronics, and payload configuration. Since it was necessary to limit the internal temperature of the payload to about 51.7° C (125° F), an aerodynamic heating analysis was conducted for this configuration. As a result of this analysis, layers of cork 0.203 cm (0.080 in.) thick were bonded to the outside surfaces of the nose cone and parachute canisters, and a layer of cork 0.318 cm (0.125 in.) thick was bonded to the outside surface of the recorder housing. To insure that the initial internal temperature of the payloads before lift-off was as low as practical, the vehicles were launched at 8:20 a.m. and 7:33 a.m., and the payload exposure to the sun was reduced to a minimum.

The internal-temperature measurements of payload 1 were made by using a thermistor located on a printed circuit board as shown in figure 7. A time history of these data is shown in figure 13. Figure 13 indicates that the internal temperature of the payload at lift-off was about 42.6° C (108.6° F) and then reduced to a minimum of about 41.9° C (107.5° F) near 8 seconds. This small temperature reduction is believed to be the result of a sudden expansion of air in the payload because of outgassing. The temperature then rose rather quickly to about 43.3° C (110° F) at 20 seconds and subsequently gradually increased to 44.4° C (112° F) at the end of the data period. A number of passive temperature sensing tabs also indicated that the maximum temperature obtained within the payloads was between 43.3° C (110° F) to 48.9° C (120° F).

Heating Rate

The external heating-rate measurements obtained from the calorimeter in flight 1 are presented in figure 14. The peak of about 26.1 kW/m^2 (2.3 Btu/ft^2-sec) at 2.4 seconds corresponds to Sidewinder burnout and maximum dynamic pressure. As is expected, the heating rate reduces during the coast phase of the flight. After Arcas ignition, the heating rate reaches a maximum of 38.02 kW/m^2 (3.35 Btu/ft^2-sec) at 27 seconds, or shortly after the maximum dynamic pressure for the Arcas burning phase.

Longitudinal Acceleration

Figure 15 presents the quasi-static longitudinal-acceleration data obtained in both flights. As is indicated by figure 15(a), ignition of the Arcas in flight 2 occurred about 0.3 second sooner and burn lasted about 3 seconds longer than for the Arcas in flight 1. In figure 15(b), the acceleration data for the first 6 seconds are shown with an expanded time scale to illustrate more clearly the accelerations during lift-off and during the burn phase of the Sidewinder. At Sidewinder rocket ignition, the acceleration builds up rapidly to at least 29.8g at 0.068 second (1g = 9.8 m/sec^2). The maximum measured level of about 32g occurs at burnout, 1.74 seconds. The acceleration remains slightly negative during Arcas coast. After Arcas ignition, the acceleration level increases to a maximum at tail-off of about 4g and 7g for flights 1 and 2, respectively, figure 15(a).

Roll Rate

The roll-rate time history of flight 2 and the theoretical pitch natural frequency (the frequency at which the vehicle oscillates due to the restoring characteristics of the aerodynamic environment) of this configuration are shown in figure 16. Roll rate was negligible until after stage separation occurred, since the first-stage fins were set at zero angle of incidence. The Arcas immediately began rolling after first-stage separation and reached a maximum of about 4.3 cps at burnout. The transient at about 23 seconds

occurs during maximum dynamic pressure for the second-stage burning and indicates possible vehicle coning motion as the vehicle approaches and passes through pitch-roll resonance. This transient is similar to that of typical Arcas pitch-roll resonance. The rapid recovery from the transient indicates good stability characteristics for this configuration.

Vibration

Longitudinal- and normal-vibration time histories are shown in figure 17 for the first 6 seconds of flight. As pointed out in table II, these data are valid over the frequency range of 20 to 2500 Hz. The amplifiers for the three channels were saturated during first- and second-stage ignition and the longitudinal channels were saturated during first-stage thrust tail-off. Therefore, the vibration data during these shock-loading periods, represented by the large amplitude changes, are not reliable. The time histories excluding the ignition and tail-off transients show that the maximum amplitudes for longitudinal vibrations are less than 1.5g and for the normal vibrations are less than 0.6g.

Samples of 1-second duration were selected for each vibration channel during first-stage thrusting (starting at 0.253 sec after first-stage ignition), second-stage coasting (starting at 3.353 sec after first-stage ignition), and second-stage thrusting (starting at 5.353 sec after first-stage ignition). The vibration data, with the exception of the rocket ignition and tail-off periods, were analyzed to determine the randomness of the data and to find periodic components in the data. A frequency resolution of 8 Hz was used during the numerical analysis of the data. Power spectral densities, histograms, and comparisons of the data with the normal distribution plots are shown in figures 18 to 26 for these selected samples.

The power-spectral-density plots have some discrete frequencies that show up as sharp spikes. The predominate frequencies shown in the power-spectral-density plots for the samples taken in the longitudinal direction are about 272 and 488 Hz for the first-stage thrusting, figures 18(a) and 19(a), respectively, and about 176 and 384 Hz for the second-stage thrusting, figures 24(a) and 25(a), respectively. The predominate frequencies for the samples taken in the normal direction are about 408, 888, and 1096 Hz during first-stage thrusting, figure 20(a), and about 688 Hz during second-stage coasting and second-stage thrusting, figures 23(a) and 26(a), respectively. The energy levels for these predominate frequencies are listed in the following table:

Event	Frequency, Hz	Power spectral density, g^2/Hz, for –		
		Lower longitudinal station	Upper longitudinal station	Normal
First-stage thrusting	272	2.55×10^{-4}	2.91×10^{-4}	----------
	408	----------	----------	8.03×10^{-5}
	488	5.31×10^{-5}	8.87×10^{-5}	----------
	888	----------	----------	1.11×10^{-4}
	1096	----------	----------	9.27×10^{-5}
Second-stage thrusting	176	9.62×10^{-5}	9.65×10^{-5}	----------
	384	4.27×10^{-5}	5.61×10^{-5}	----------
	688	----------	----------	2.24×10^{-4}
Second-stage coasting	688	----------	----------	3.33×10^{-4}

The histogram and probability plots indicate some deviations from a Gaussian distribution. However, the fitted normal distributions shown in the (c) parts of figures 18 to 20 and figures 24 to 26 approximate the measured distribution during thrusting quite well except at the large negative and positive values of g. The data sampled during second-stage coasting indicate that the normal distribution adequately predicts the vibration during this period, (c) parts of figures 21 to 23.

CONCLUDING REMARKS

Two Sidewinder-Arcas rockets were flight tested to measure some flight-induced environments to which research payloads would be subjected when flight tested on this vehicle configuration. The data obtained were acceleration, structural vibration, internal temperature, heating rate, and roll rate. The data indicate that the maximum quasi-static longitudinal acceleration is about 32g and occurs at first-stage thrusting tail-off ($1g = 9.8\ m/sec^2$). The maximum vibrations measured, excluding the vibrations during rocket ignition and tail-off, have amplitudes less than 1.5g for the longitudinal or thrust axis and less than 0.6g for the normal axis. The thermal data indicate that the maximum payload internal temperature is 44.4° C (112° F) and that the maximum heat rate is 38 kW/m^2 (3.35 Btu/ft^2-sec). The second stage reached a maximum roll rate of 4.3 cps at second-stage burnout.

Langley Research Center,
National Aeronautics and Space Administration,
Hampton, Va., September 14, 1971.

REFERENCE

1. Anon.: U.S. Standard Atmosphere Supplements, 1966. Environ. Sci. Serv. Admin., NASA, and U.S. Air Force.

TABLE I.- SYSTEM WEIGHTS

Event	Sidewinder with interstage		Arcas		Parachute		Payload		Total	
	kg	lb	kg	lb	kg	lb	kg	lb	kg	lb
Flight 1										
Lift-off	42.4	93.5	31.41	69.25	2.10	4.63	6.24	13.75	82.16	181.13
First-stage burnout	22.81	50.29	↓	↓	↓	↓	↓	↓	62.56	137.92
Second-stage ignition	↓	↓	↓	↓	↓	↓	↓	↓	39.75	87.63
Second-stage burnout	↓	↓	11.86	26.15	↓	↓	↓	↓	20.20	44.53
Flight 2										
Lift-off	42.4	93.5	31.41	69.25	2.10	4.63	6.26	13.81	82.19	181.19
First-stage burnout	22.81	50.29	↓	↓	↓	↓	↓	↓	62.59	137.98
Second-stage ignition	↓	↓	↓	↓	↓	↓	↓	↓	39.78	87.69
Second-stage burnout	↓	↓	11.86	26.15	↓	↓	↓	↓	20.23	44.59

TABLE II.- PAYLOADS

	Payload 1	Payload 2
Length	82.0 cm (32.3 in.)	82.0 cm (32.3 in.)
Diameter at base	11.2 cm (4.4 in.)	11.2 cm (4.4 in.)
Tape recorder	Raymond model 1849	Raymond model 1849
Tape speed	38.1 cm/sec (15 in./sec)	38.1 cm/sec (15 in./sec)
Run time	90 sec	90 sec
Recorder technique	Wideband FM	Wideband FM
Recorder frequency response	100 to 25 000 Hz ± 3 dB	100 to 25 000 Hz ± 3 dB
Longitudinal acceleration	Piezoresistive, Endevco Model 2260; Range: 0g to 125g; System frequency response: 0 to 2.5 kHz	Nonpendulous servo accelerometer; Kistler Model 303; Range: -5g to +35g; System frequency response: 0 to 1 kHz
Heating rate	Asymptotic calorimeter, Hy-Cal, model C-1104-C-ZZ-XXX-YYY; Range: 0 to 227 kW/m^2 (0 to 20 Btu/ft^2-sec)	
Internal heating	Thermistor; Range: 10^{o} C to 93^{o} C (50^{o} to 200^{o} F)	
Roll rate		Nonpendulous servo accelerometer; Kistler Model 303; Range: 0 to 600 rpm; System frequency response: 0 to 20 Hz
Longitudinal vibration		Quartz accelerometer; Kistler Model 808H; Charge amplifier, Kistler Model 553A; System frequency response: 20 to 2500 Hz Range: ±5g
Normal vibration		Quartz accelerometer; Kistler Model 808H; Charge amplifier, Kistler Model 553A; System frequency response: 20 to 2500 Hz Range: ±2.5g

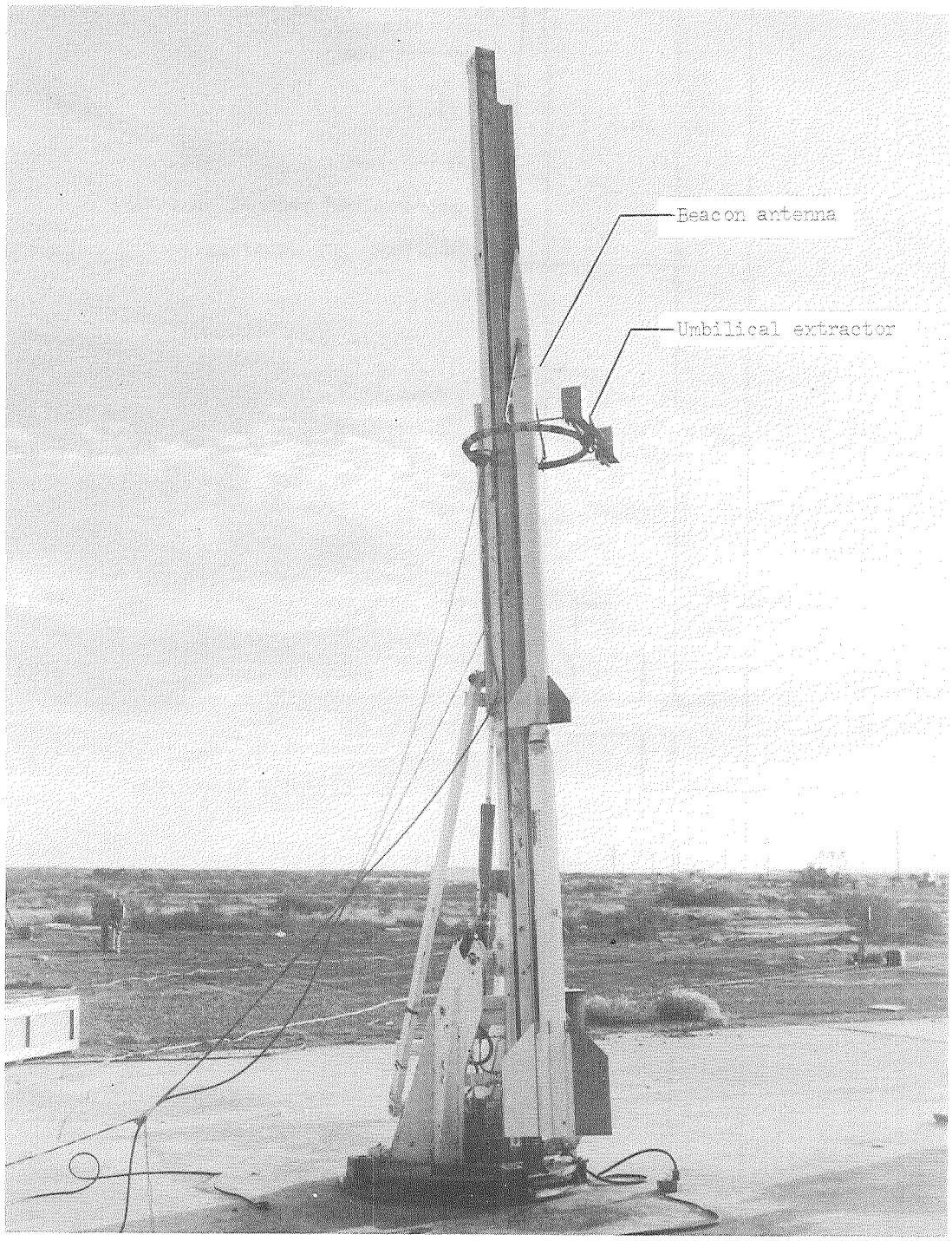

Figure 1.- Sidewinder-Arcas sounding rocket on launcher. U.S. Army photograph.

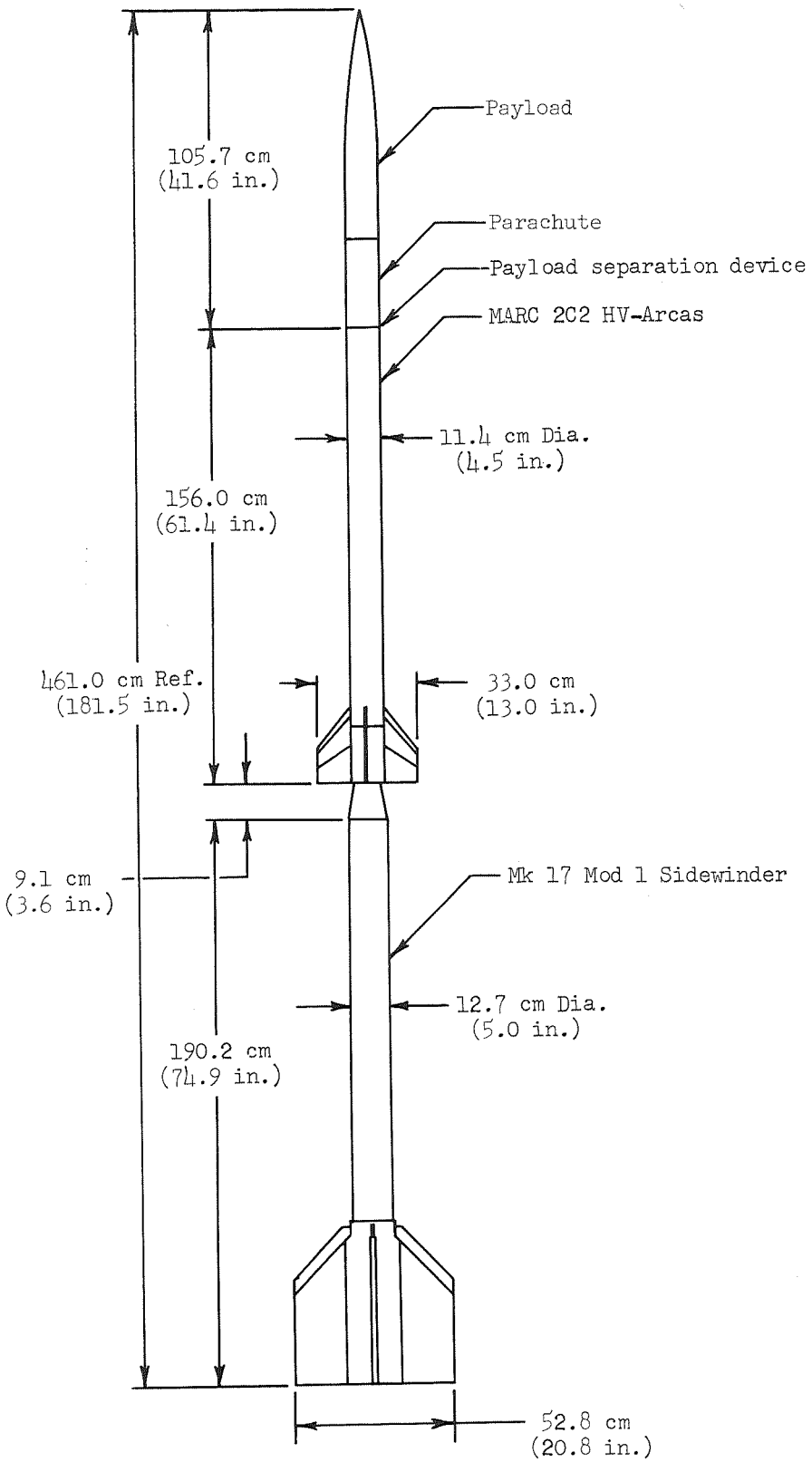

Figure 2.- Sidewinder-Arcas sounding rocket.

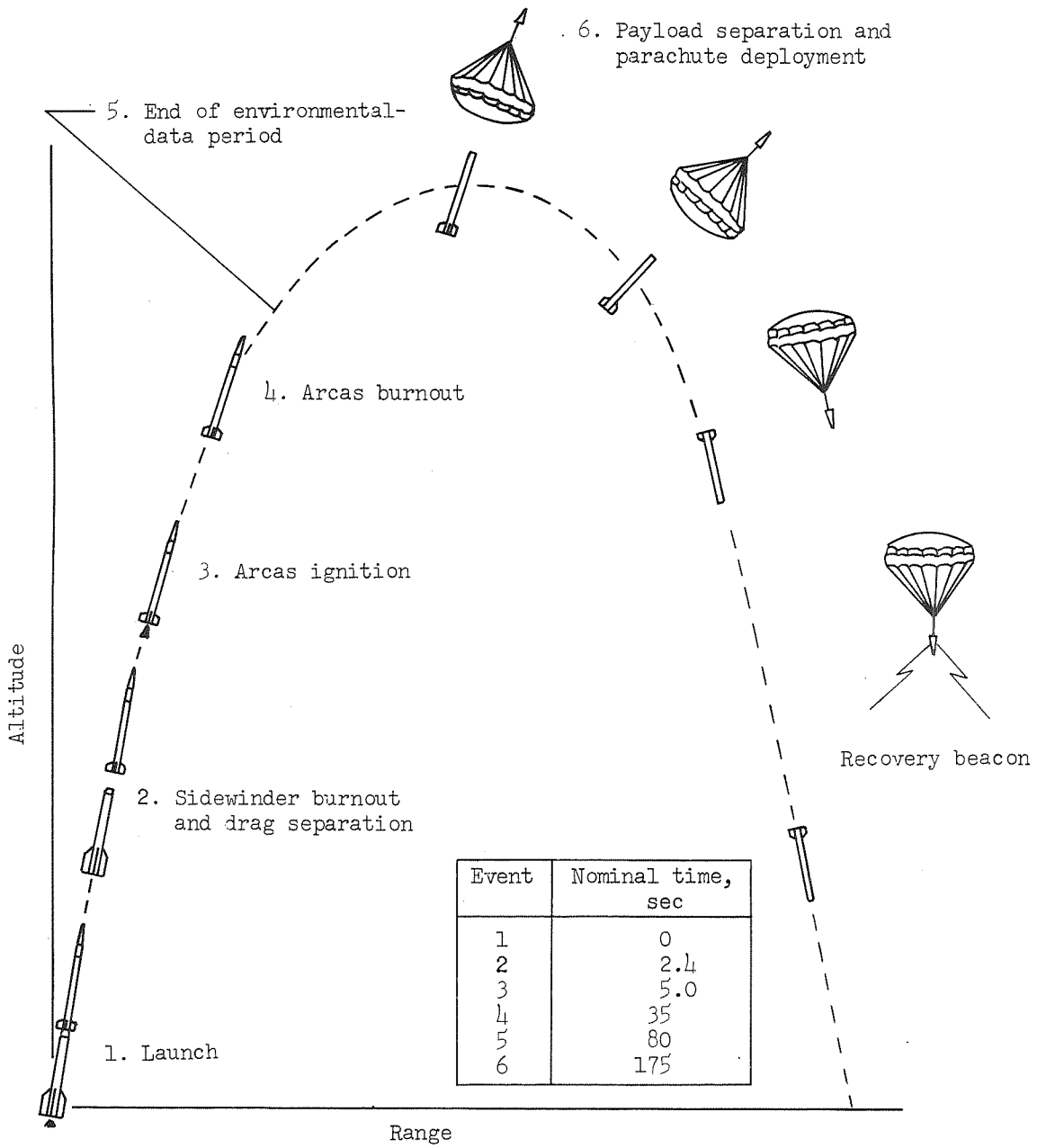

Event	Nominal time, sec
1	0
2	2.4
3	5.0
4	35
5	80
6	175

Figure 3.- Mission profile.

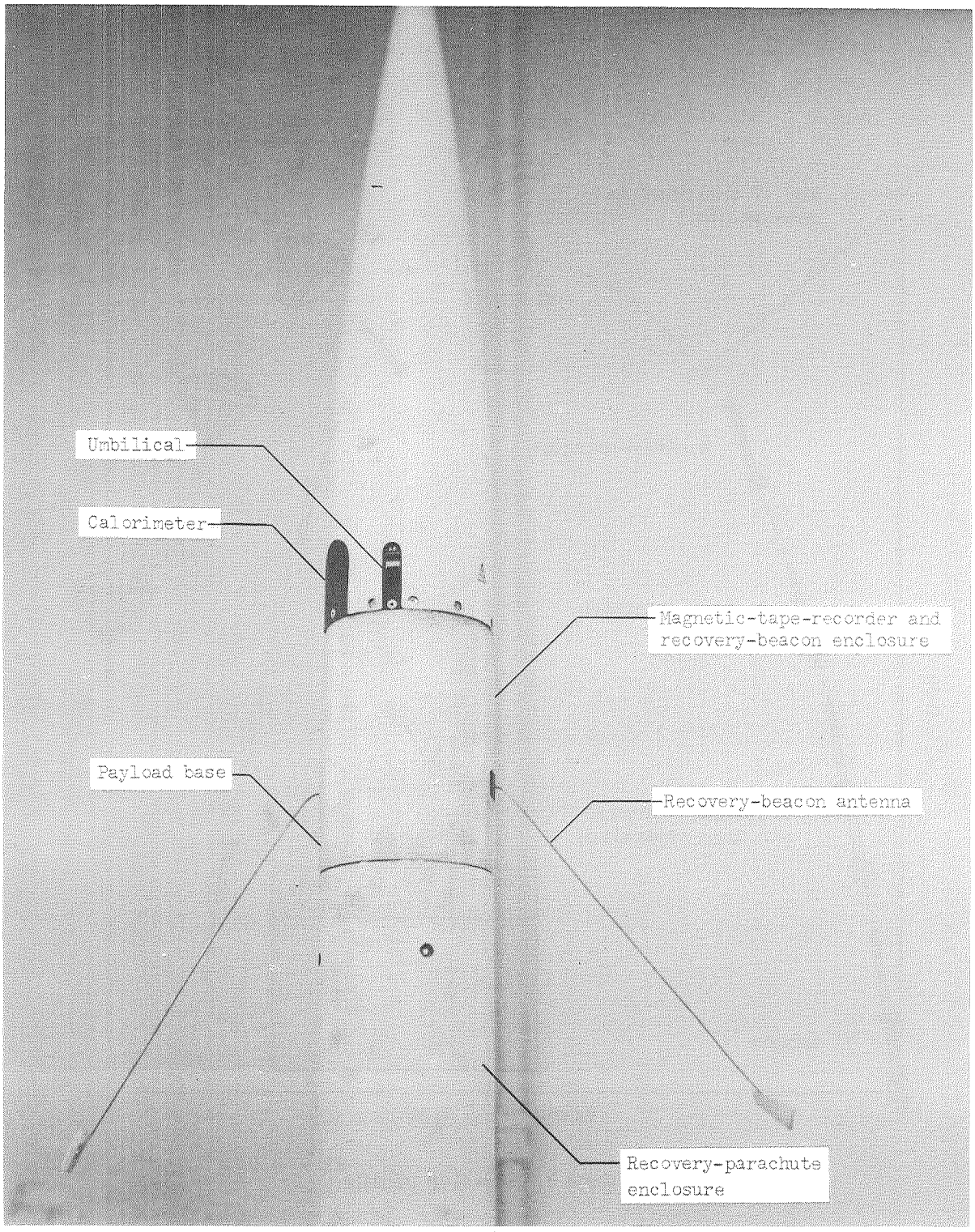

Figure 4.- Environmental payload. U.S. Army photograph.

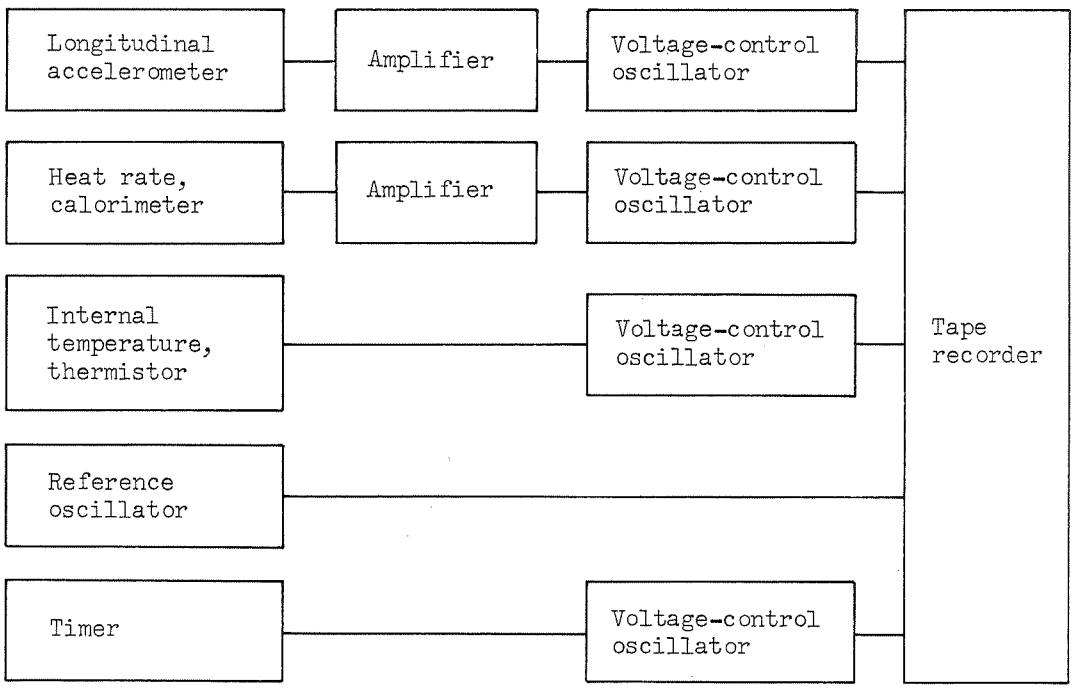

Figure 5.- Instrumentation block diagram for payload 1.

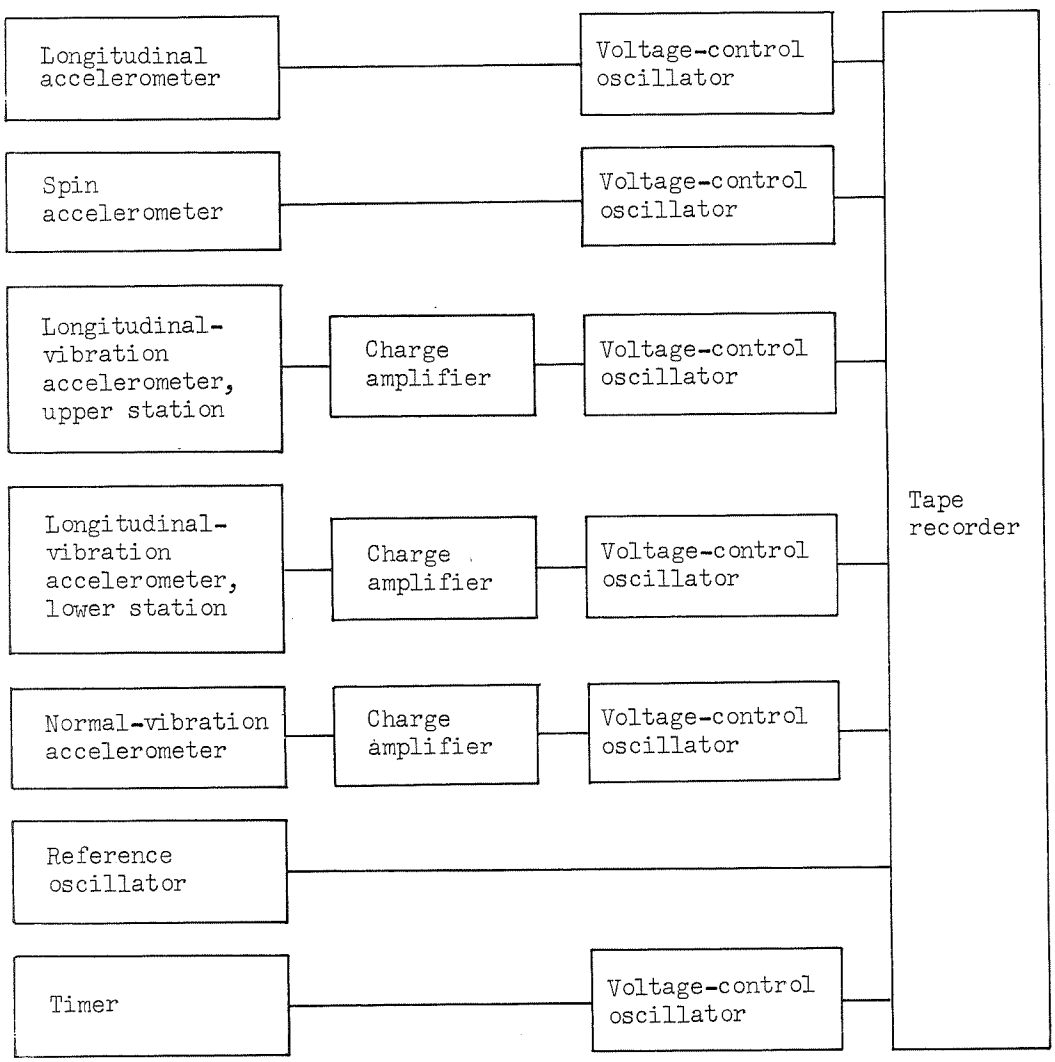

Figure 6.- Instrumentation block diagram for payload 2.

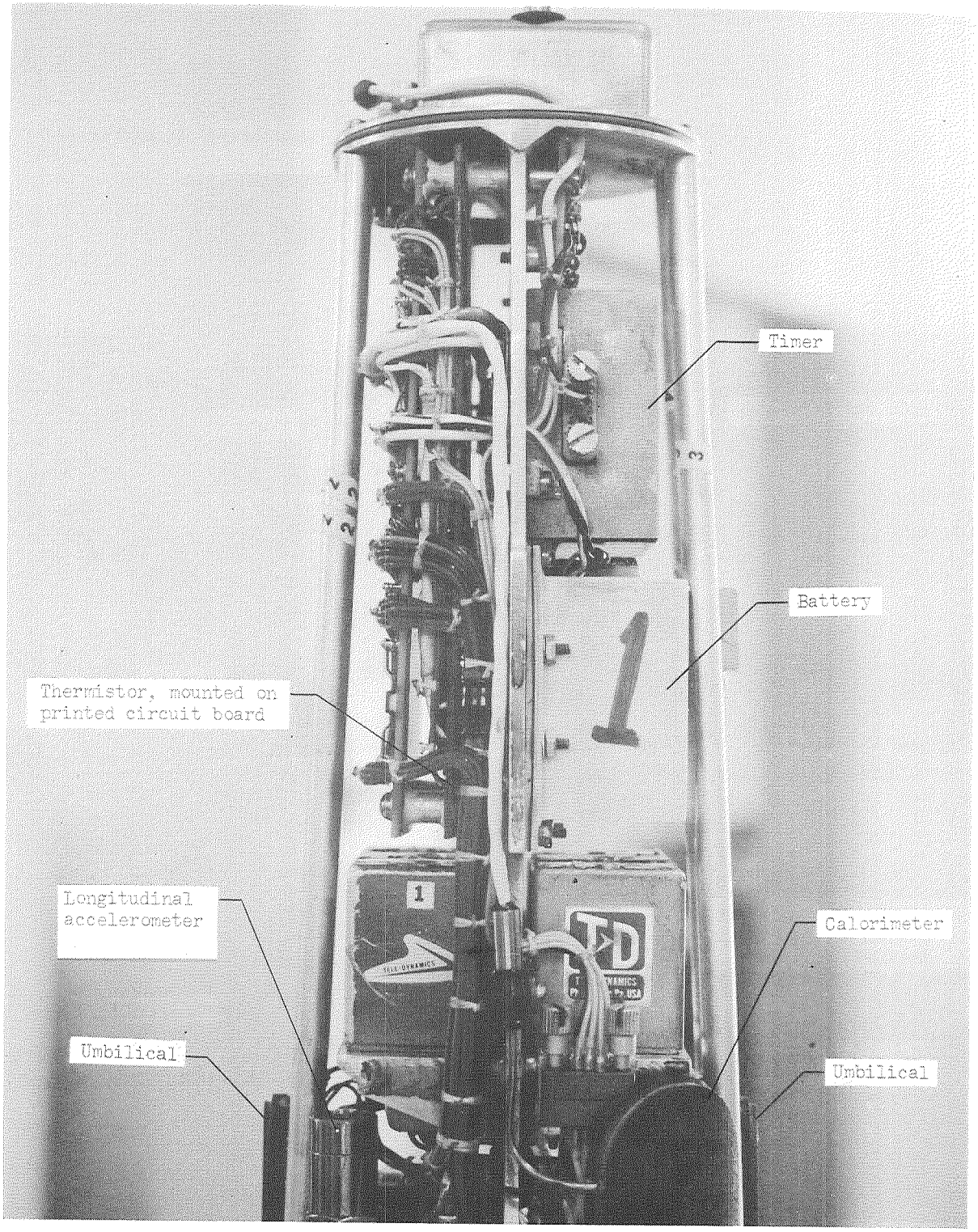

Figure 7.- Payload 1. U.S. Army photograph.

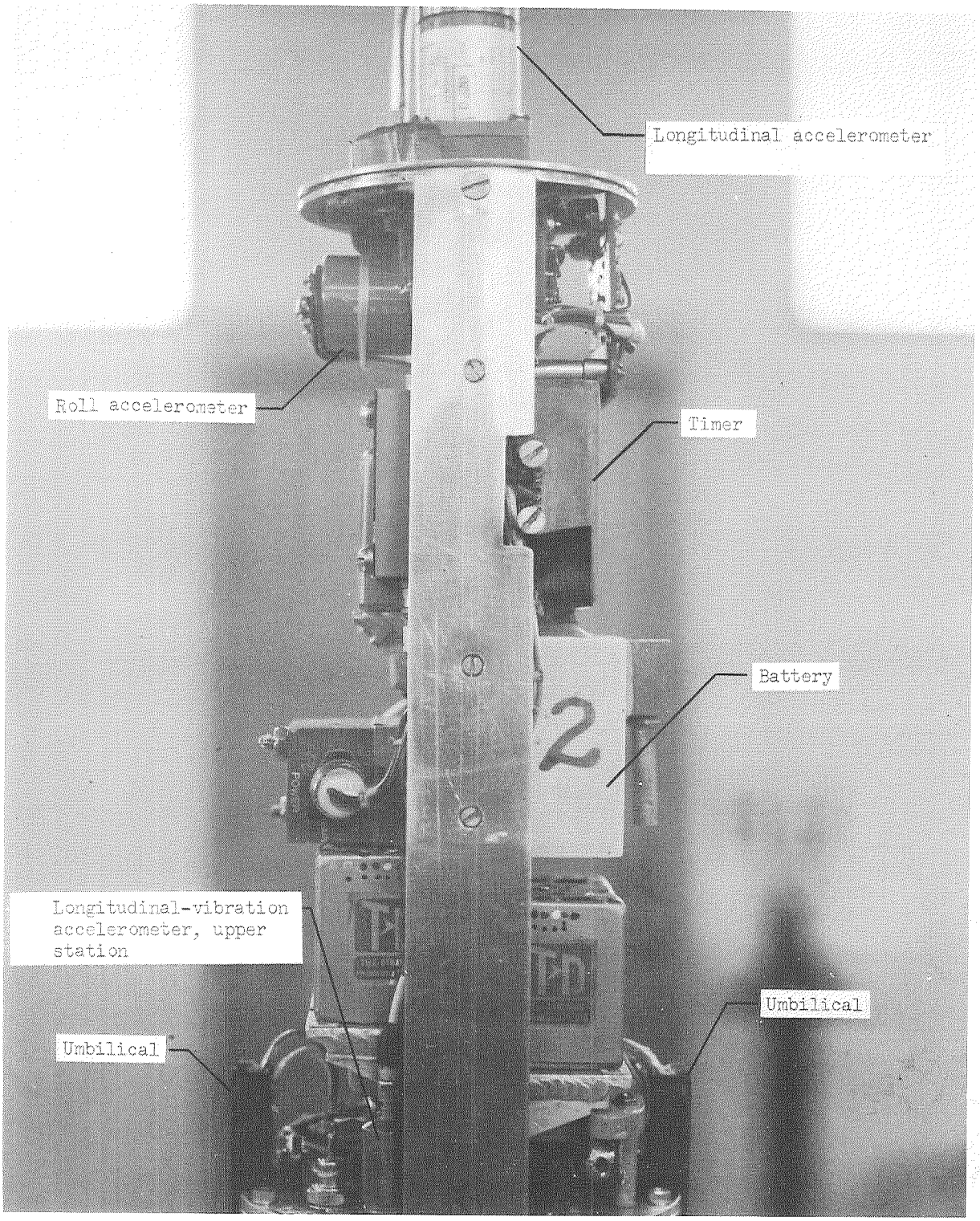

(a) Instrument locations. U.S. Army photograph.

Figure 8.- Payload 2.

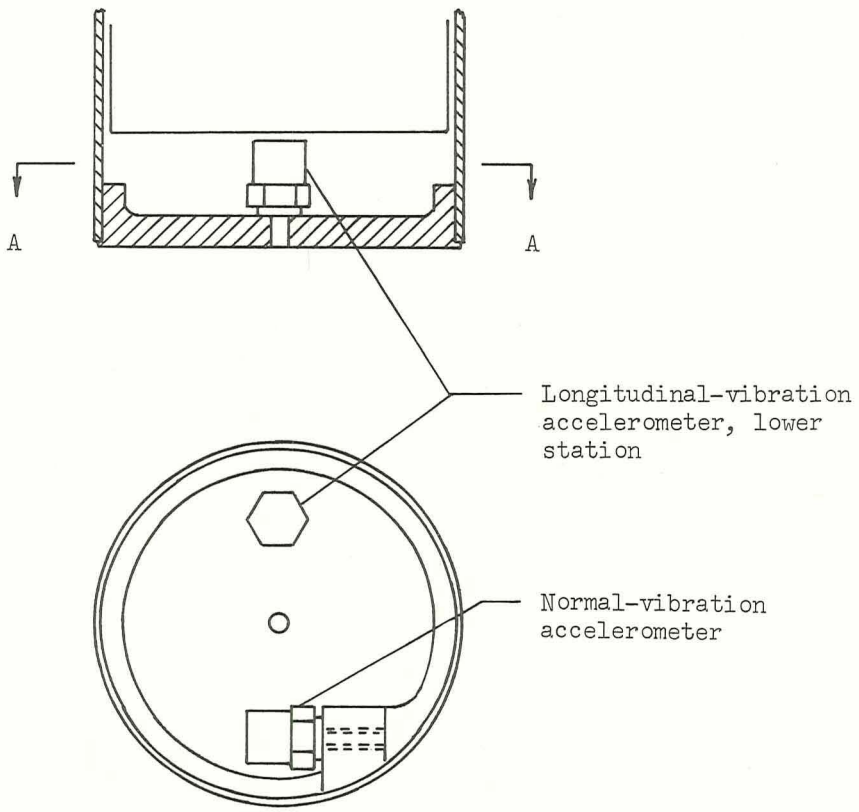

Section A-A

(b) Base section.

Figure 8.- Concluded.

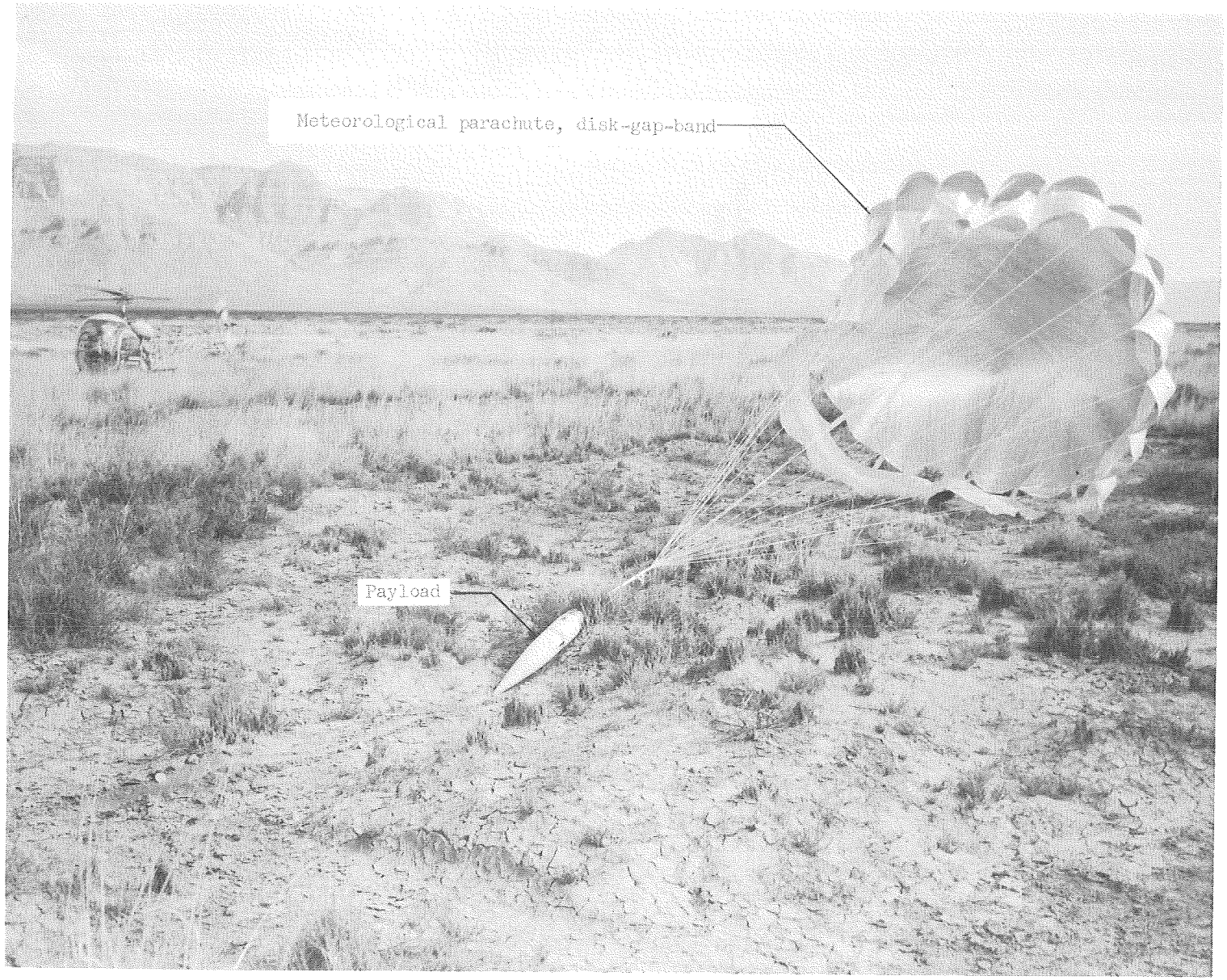

Figure 9.- Payload recovery. U.S. Army photograph.

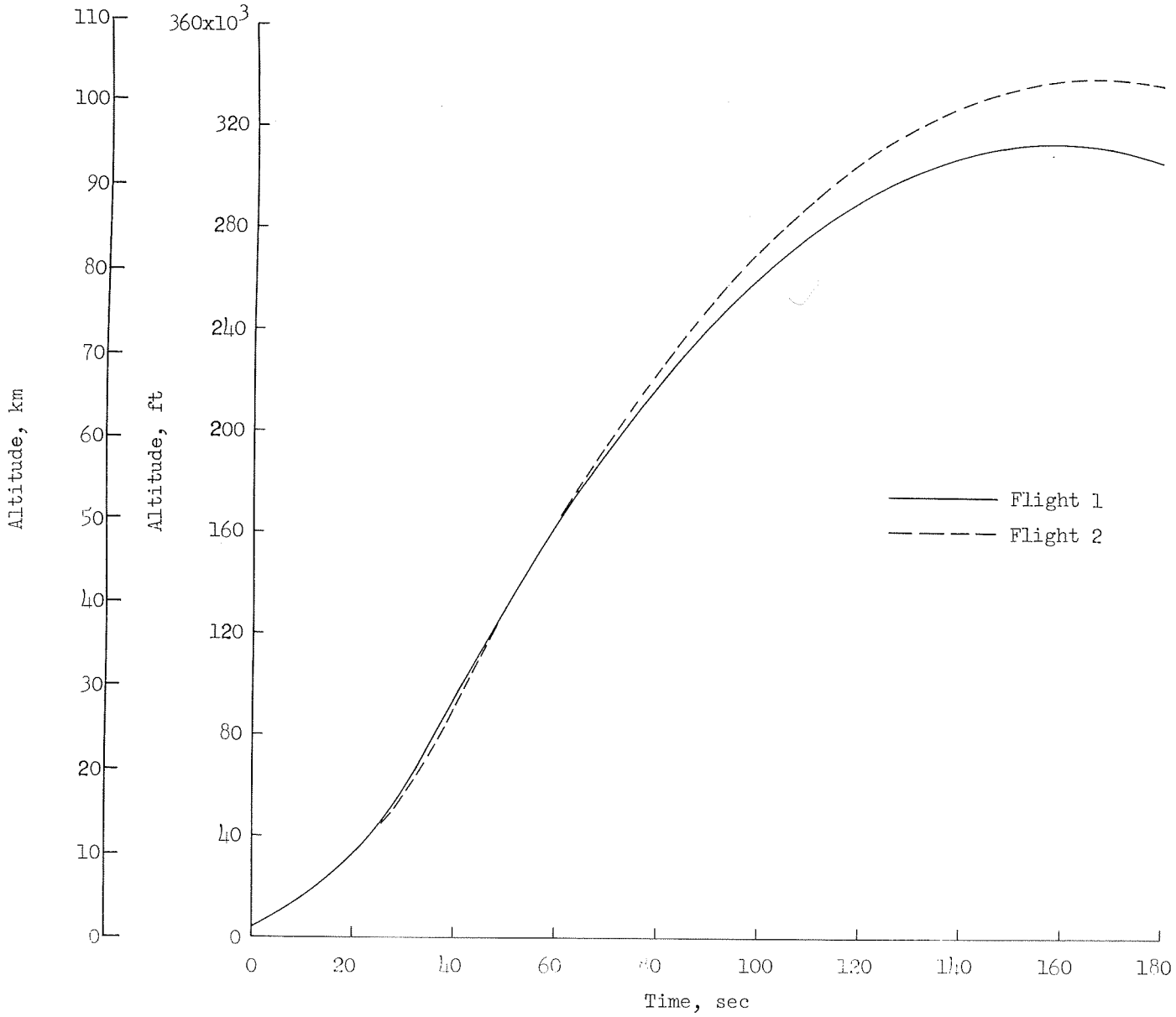

Figure 10.- Altitude time history.

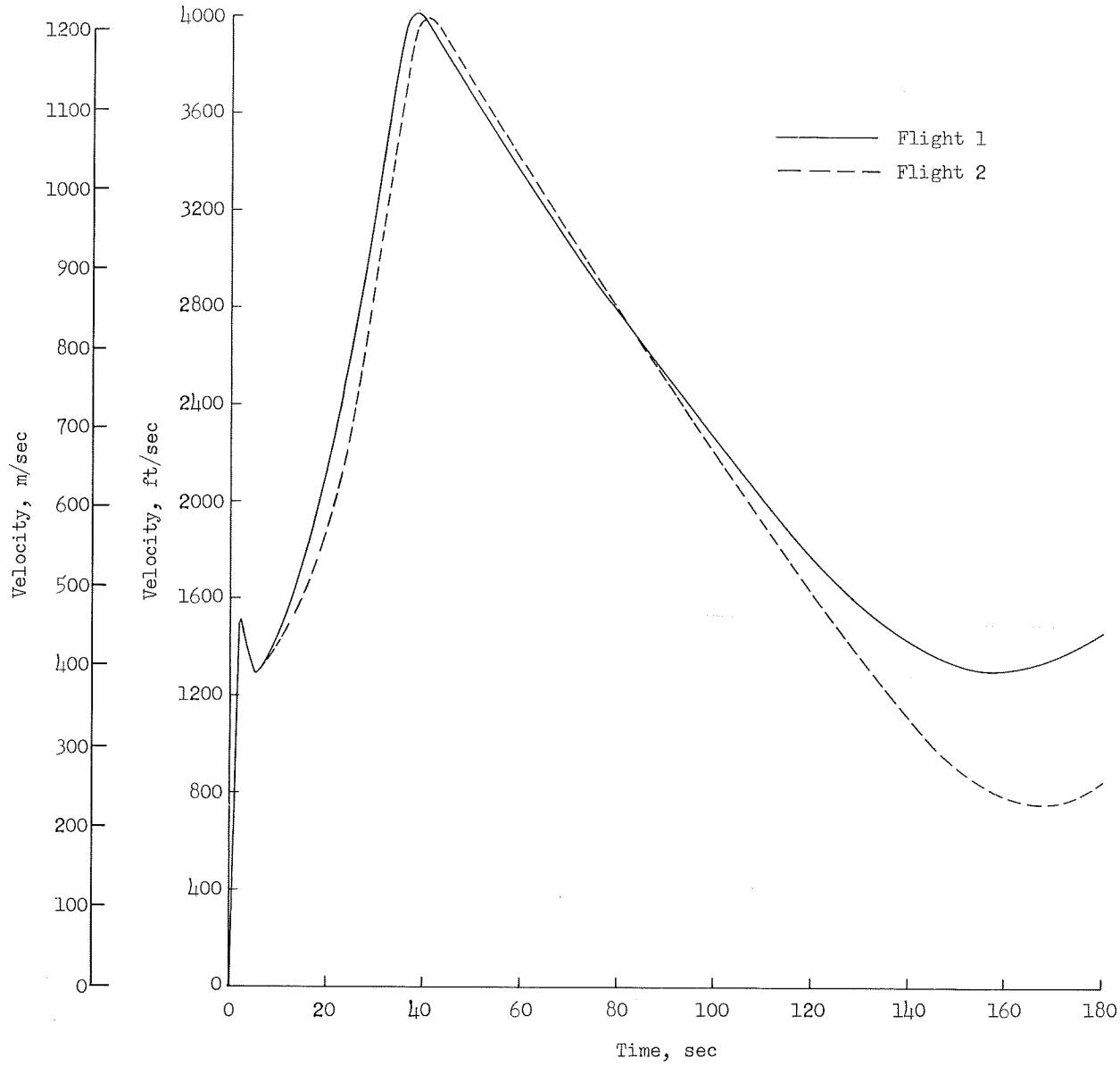

Figure 11.- Velocity time history.

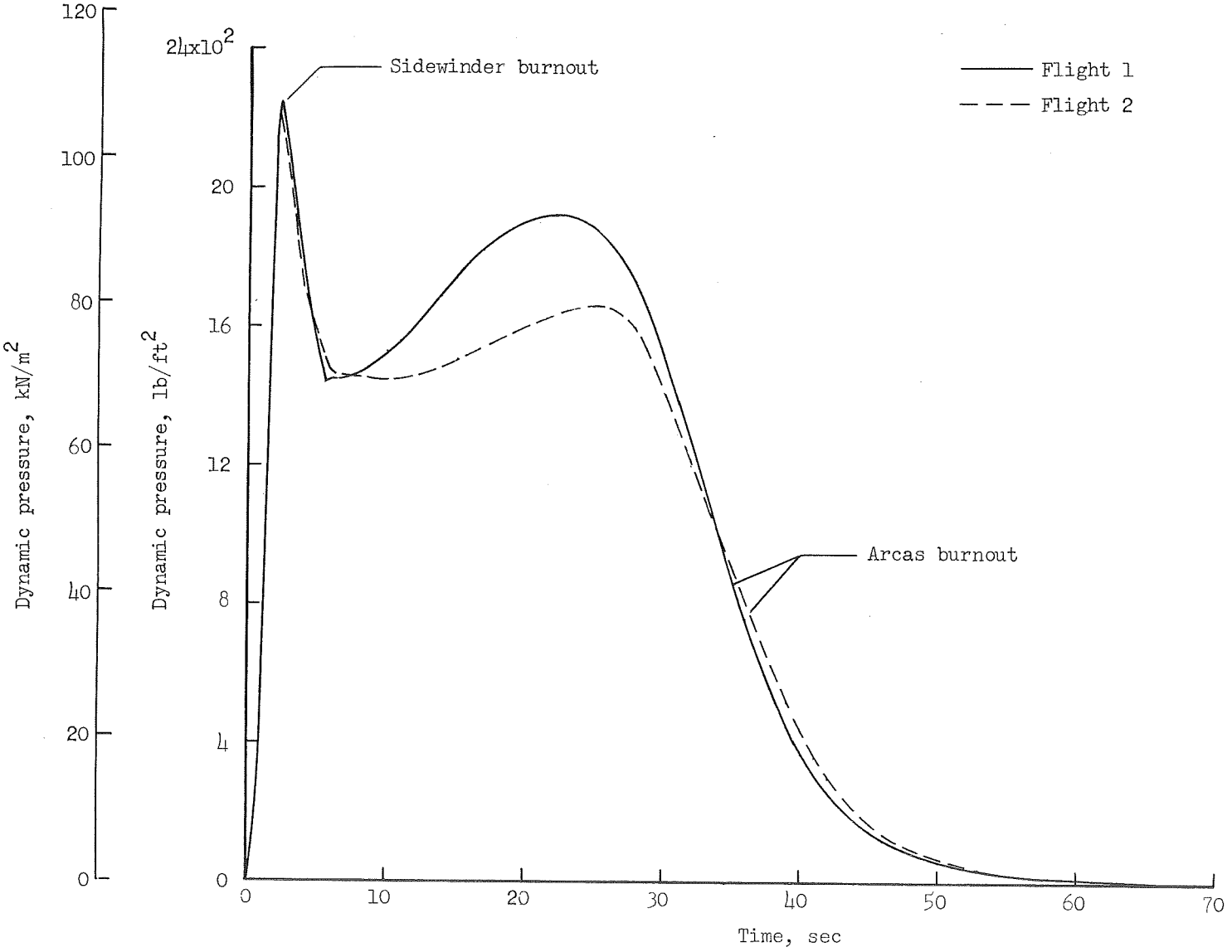

Figure 12.- Dynamic-pressure time history. (Density used in computation from ref. 1 for 30° N lat, July.)

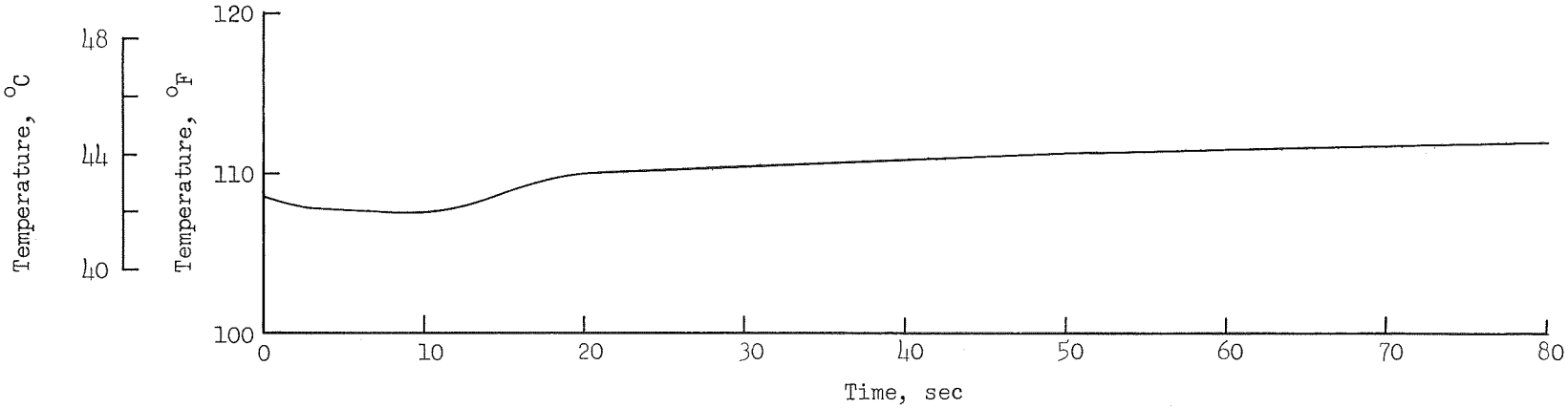

Figure 13.- Payload 1 internal-temperature time history. Flight 1.

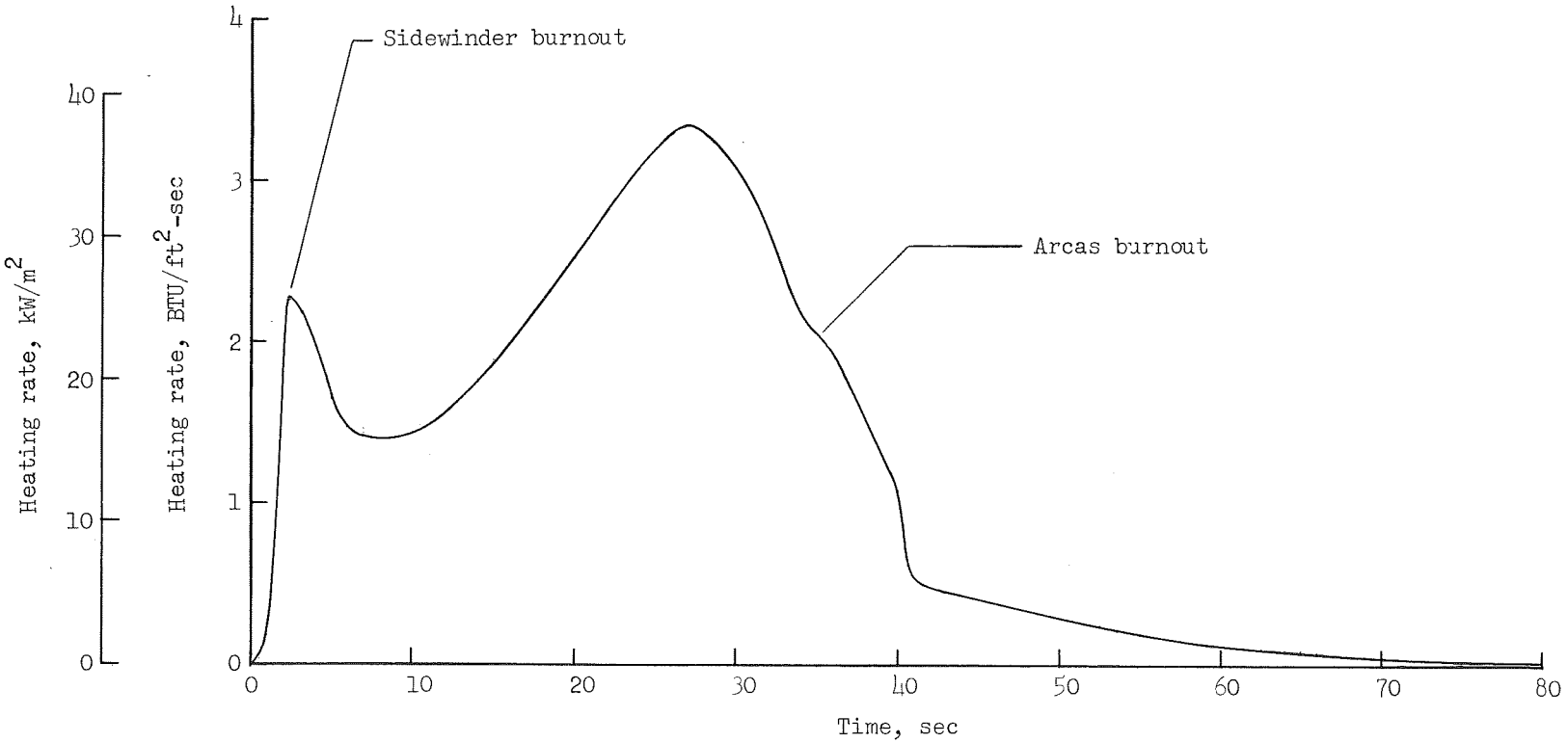

Figure 14.- Heating-rate time history. Flight 1.

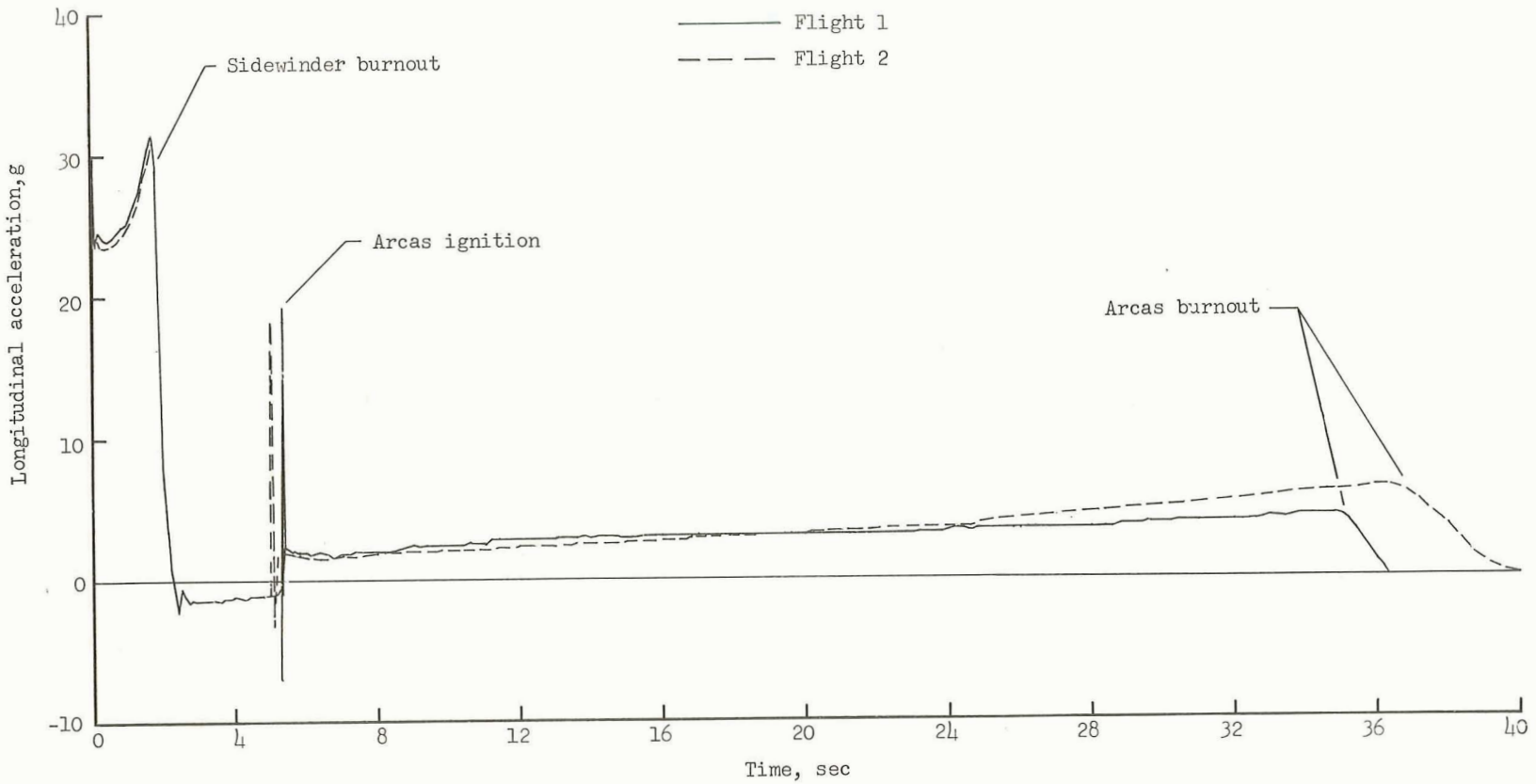

(a) From 0 to 40 sec.

Figure 15.- Longitudinal-acceleration time history.

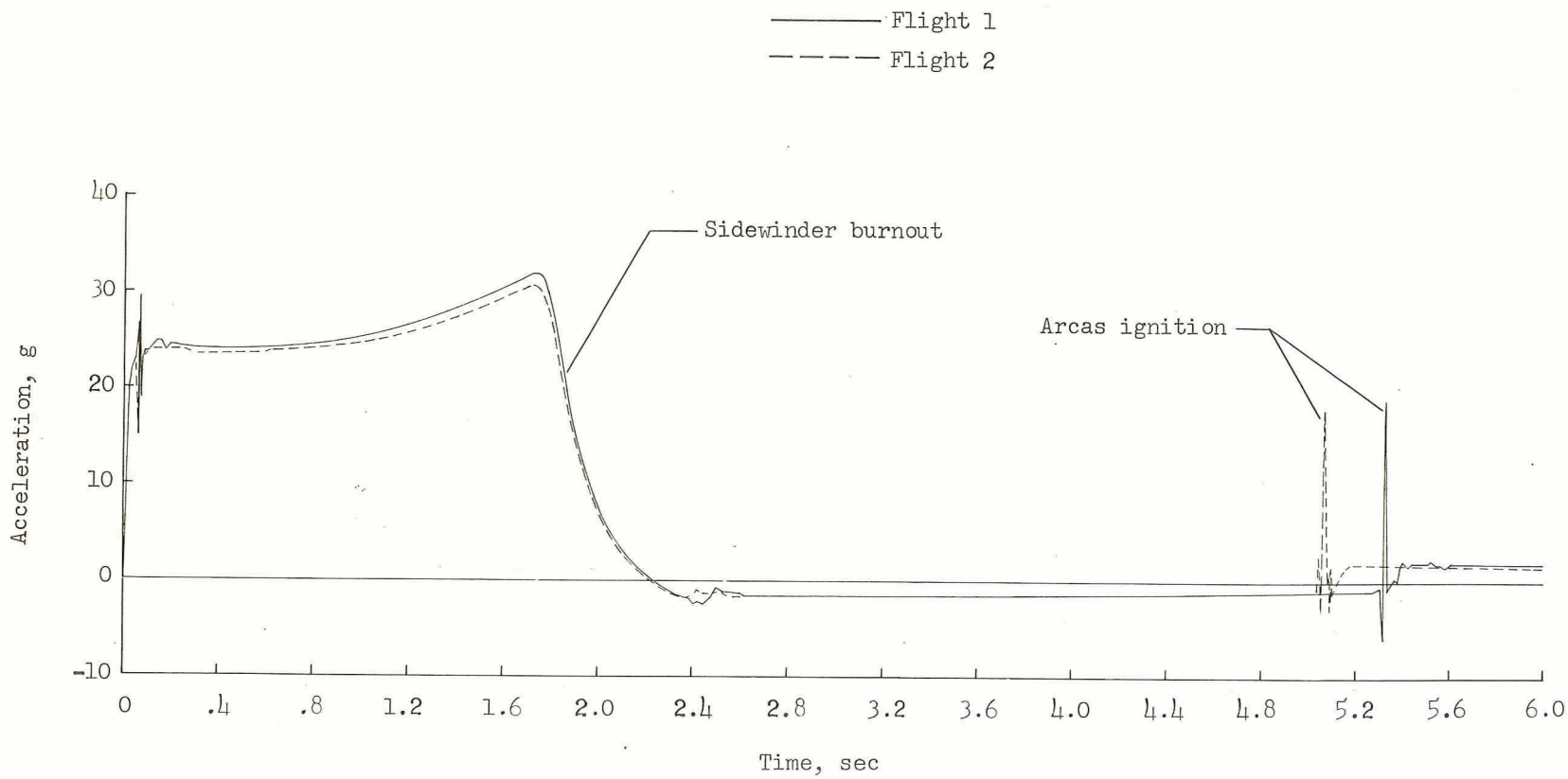

(b) From 0 to 6 sec (expanded scale).

Figure 15.- Concluded.

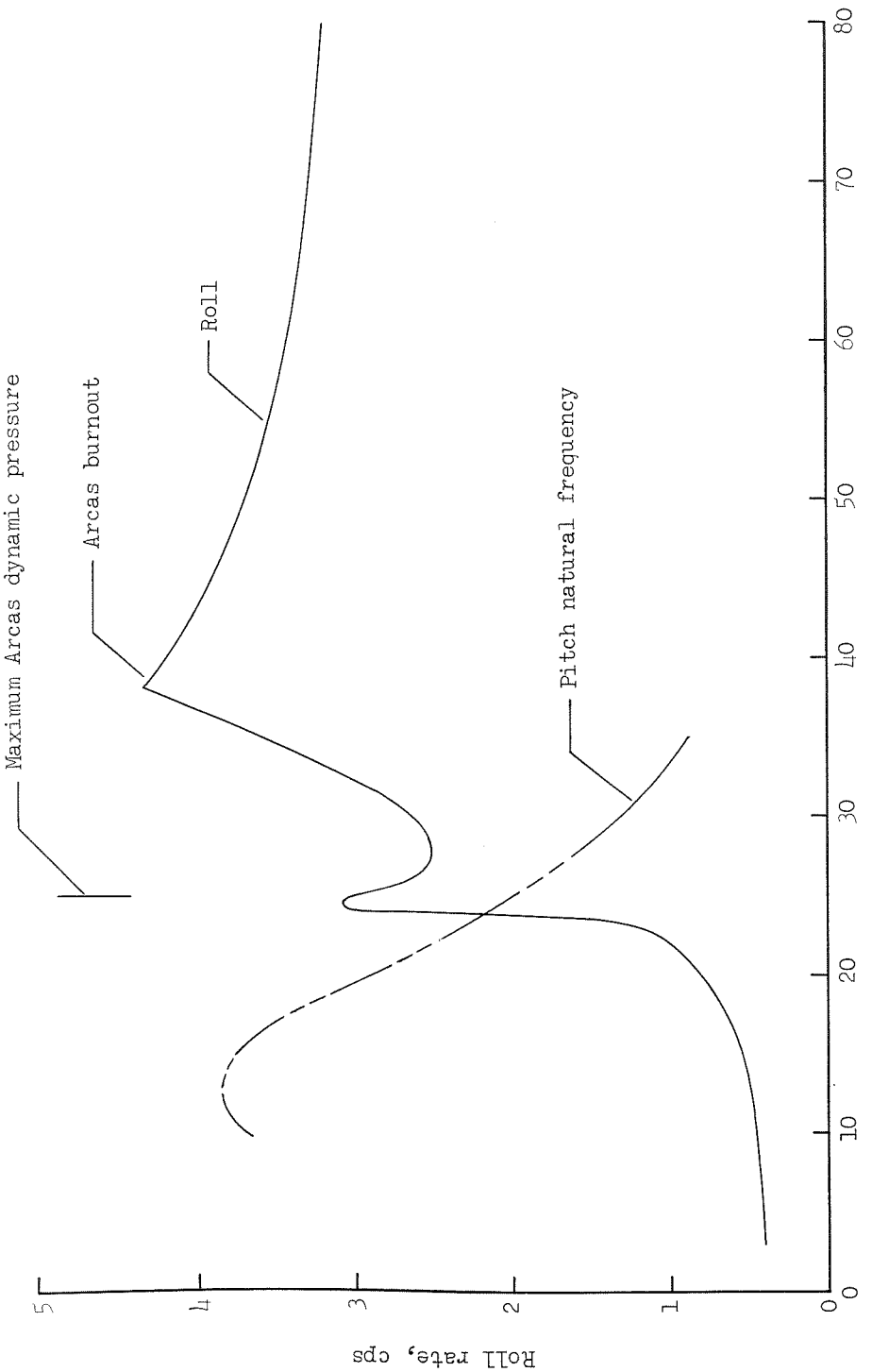

Figure 16.- Roll-rate time history. Flight 2.

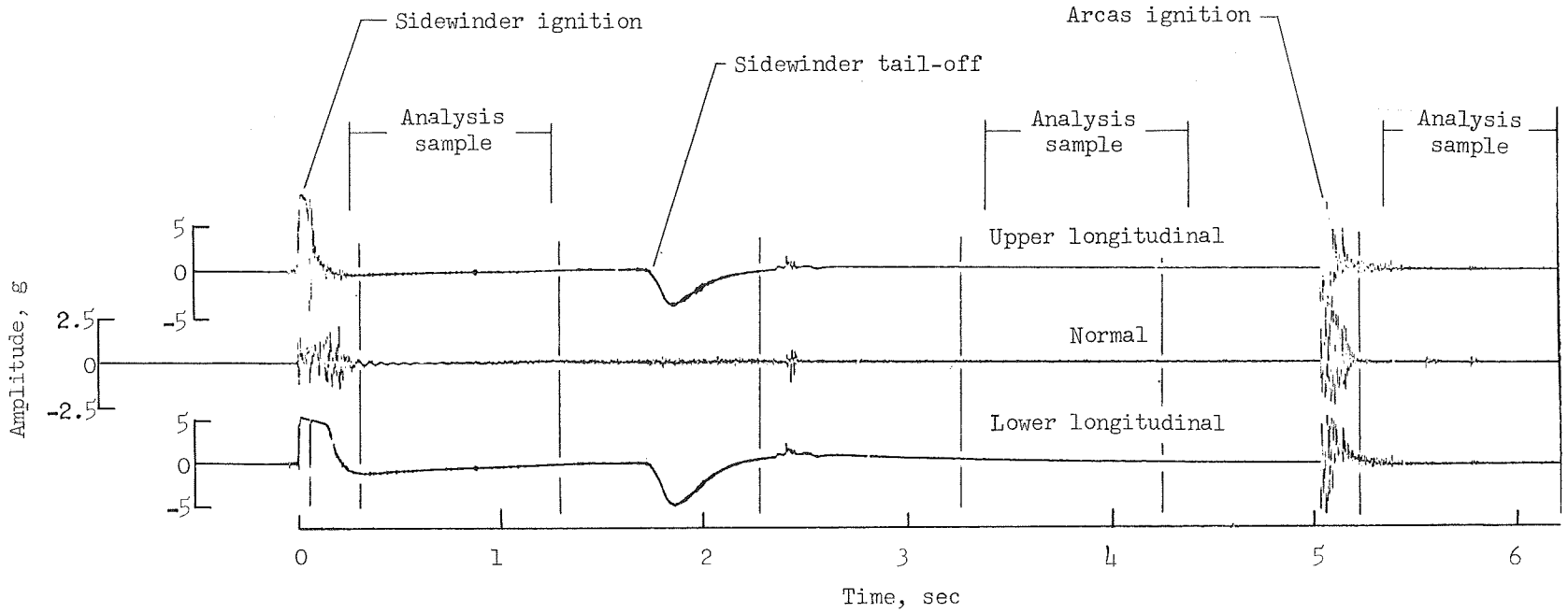

Figure 17.- Vibration time histories for first 6 seconds of flight.

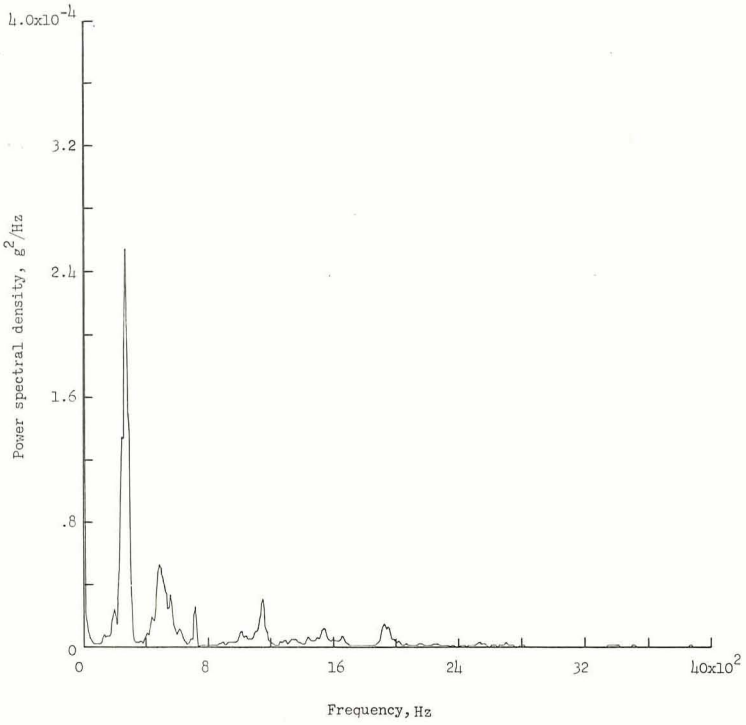

(a) Power spectral density.

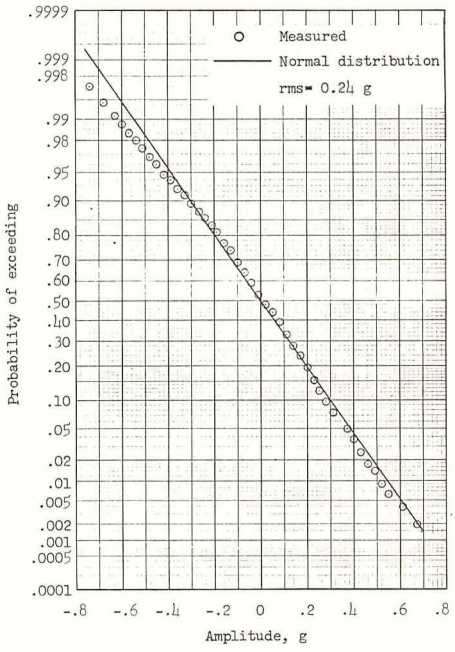

(c) Probability of equaling or exceeding given values of g.

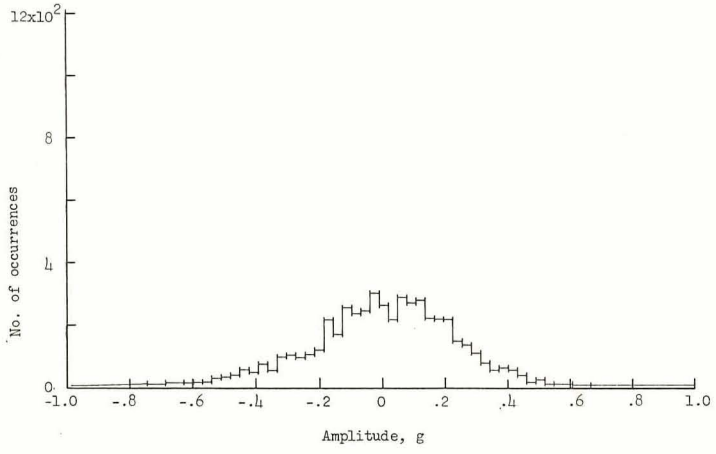

(b) Histogram.

Figure 18.- Lower longitudinal vibration of 1-second sample starting at 0.253 second after first-stage ignition.

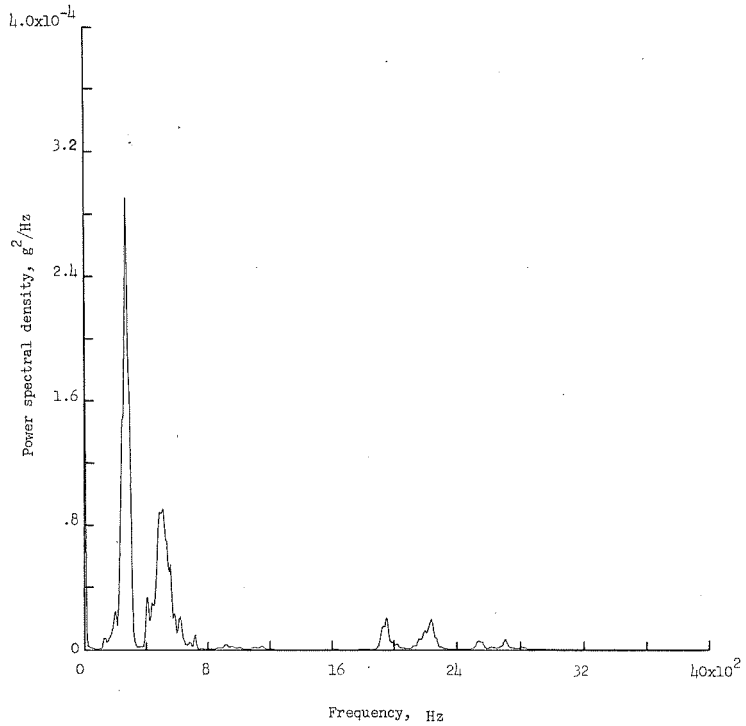

(a) Power spectral density.

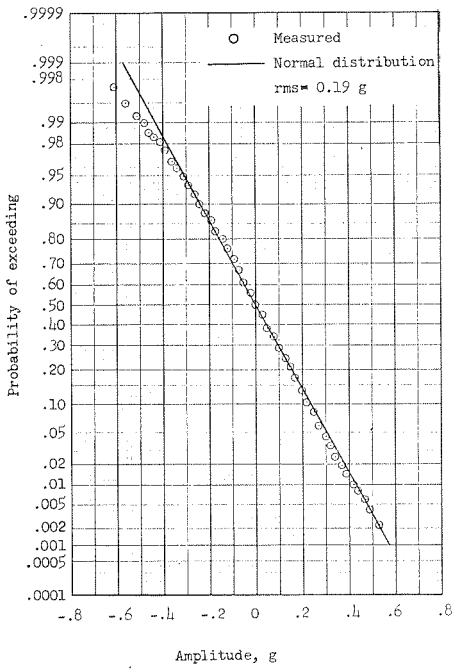

(c) Probability of equaling or exceeding given values of g.

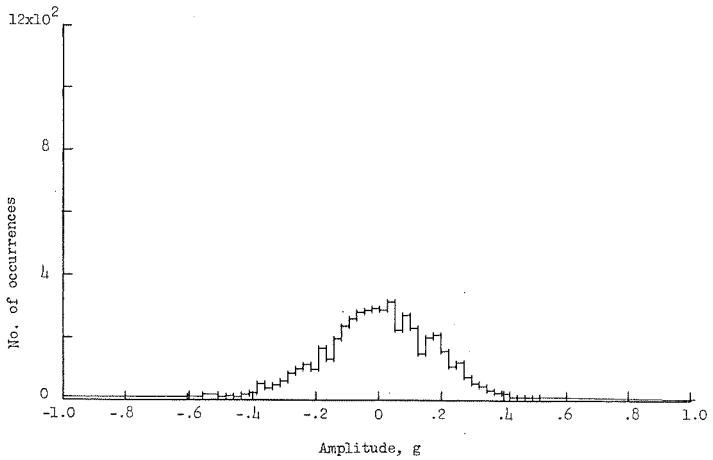

(b) Histogram.

Figure 19.- Upper longitudinal vibration of 1-second sample starting at 0.253 second after first-stage ignition.

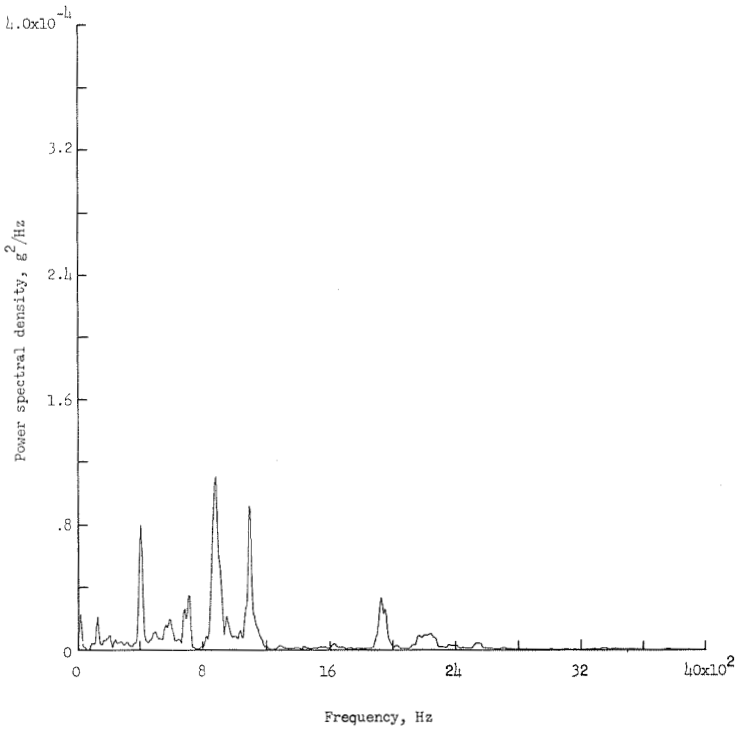

(a) Power spectral density.

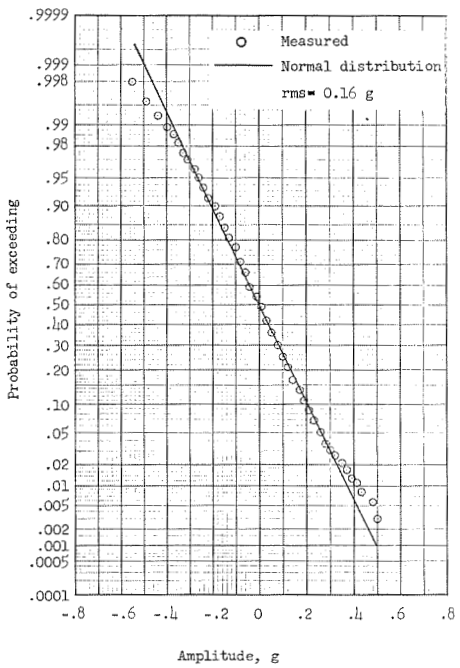

(c) Probability of equaling or exceeding given values of g.

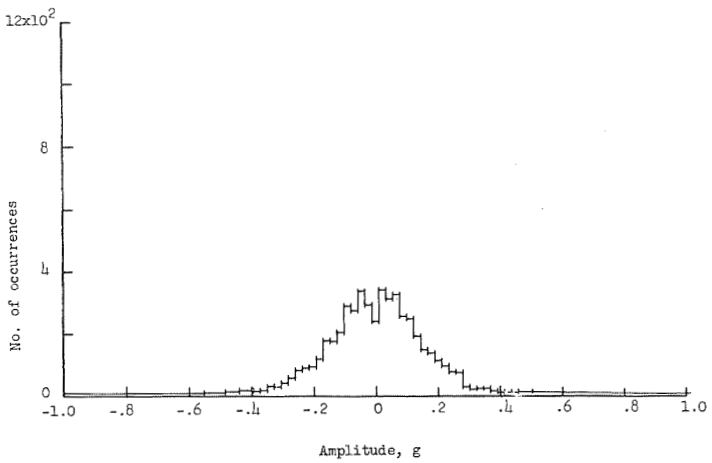

(b) Histogram.

Figure 20.- Normal vibration of 1-second sample starting at 0.253 second after first-stage ignition.

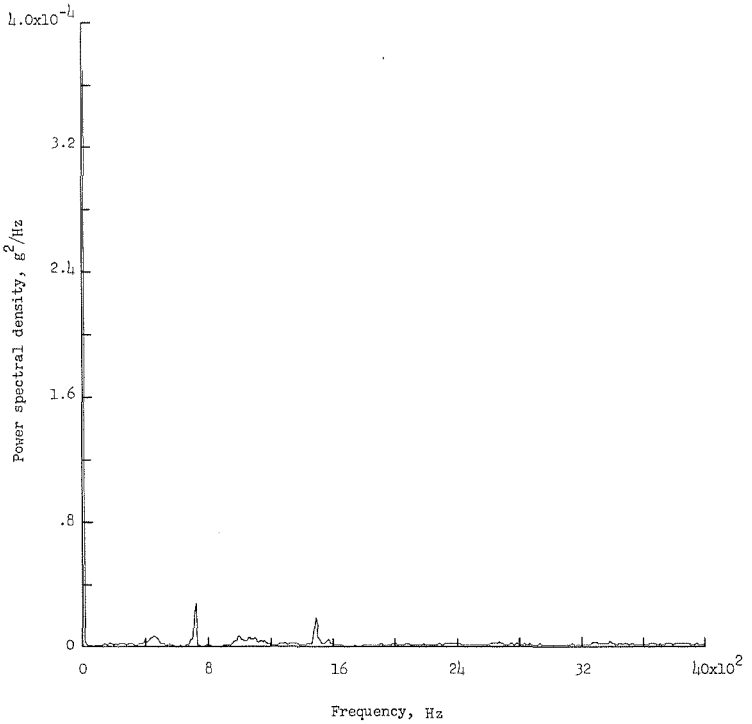

(a) Power spectral density.

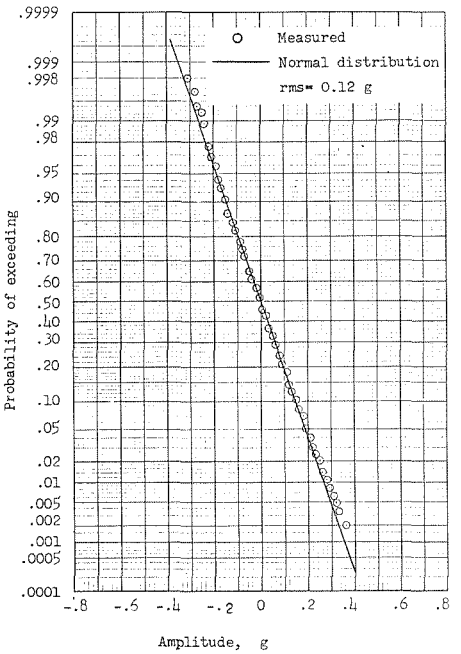

(c) Probability of equaling or exceeding given values of g.

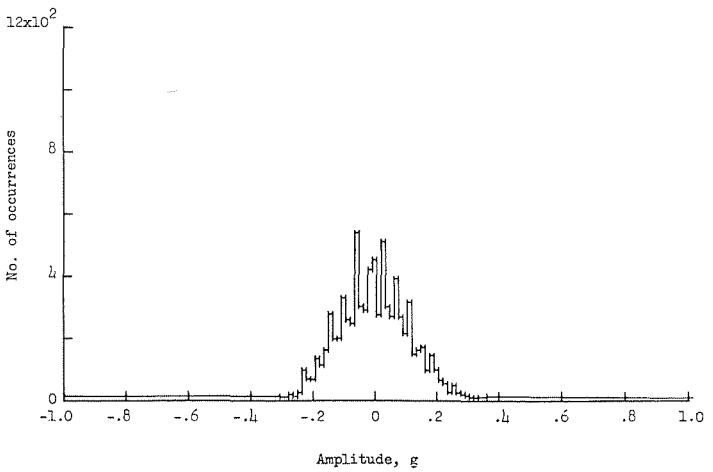

(b) Histogram.

Figure 21.- Lower longitudinal vibration of 1-second sample starting at 3.353 seconds after first-stage ignition.

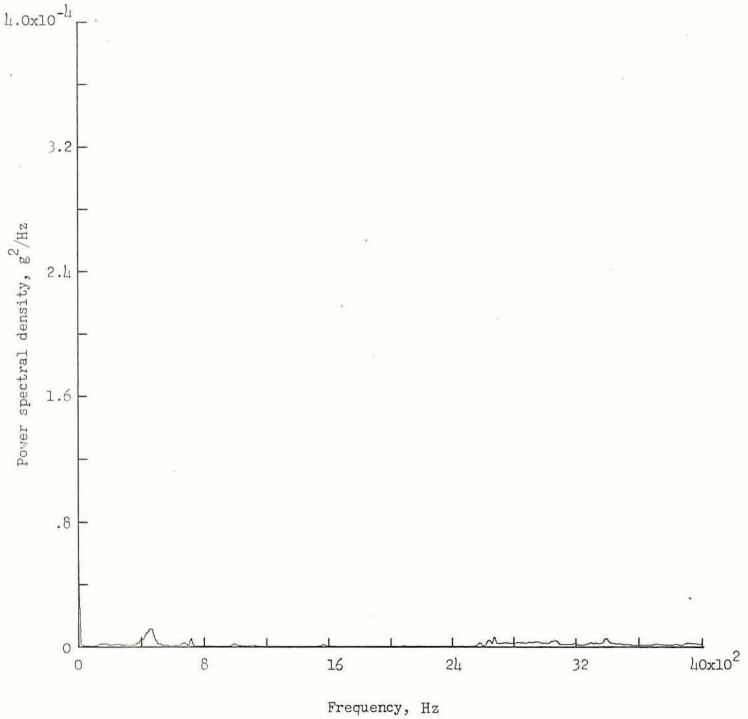

(a) Power spectral density.

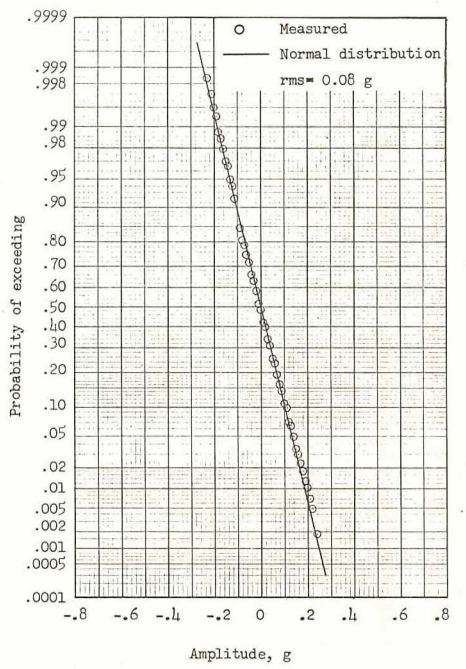

(c) Probability of equaling or exceeding given values of g.

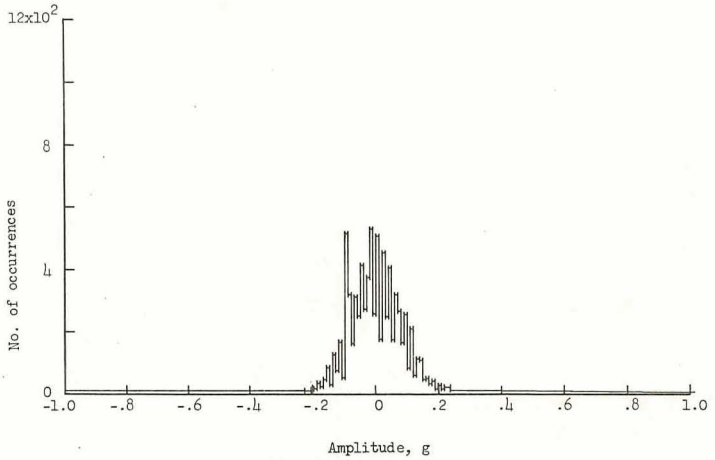

(b) Histogram.

Figure 22.- Upper longitudinal vibration of 1-second sample starting at 3.353 seconds after first-stage ignition.

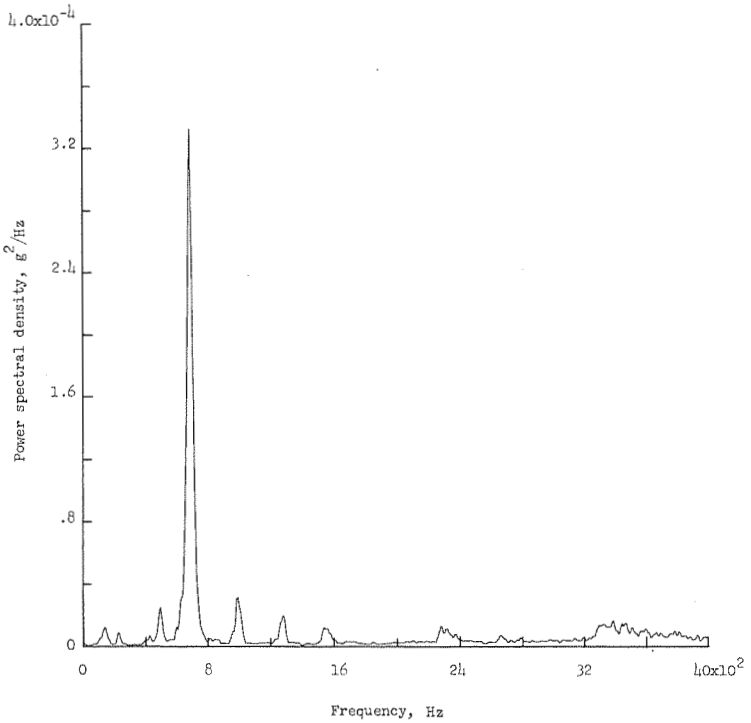

(a) Power spectral density.

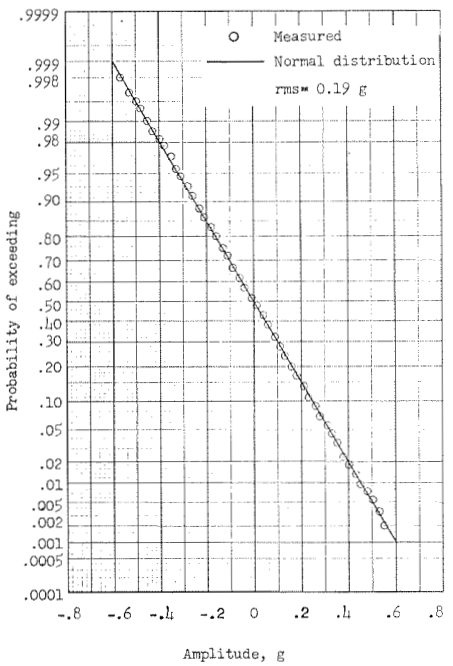

(c) Probability of equaling or exceeding given values of g.

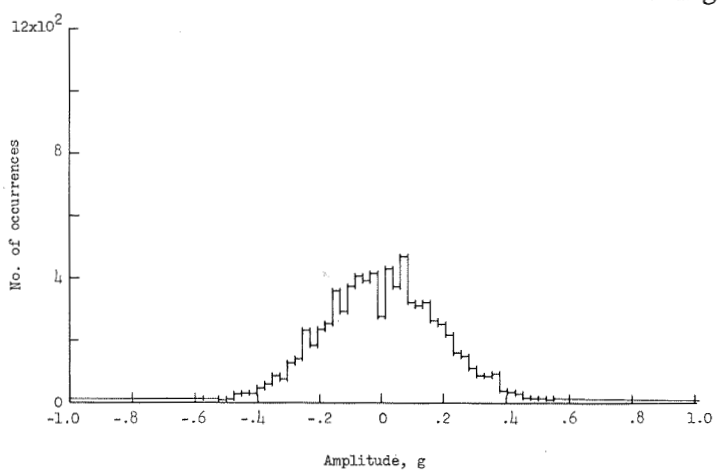

(b) Histogram.

Figure 23.- Normal vibration of 1-second sample starting at 3.353 seconds after first-stage ignition.

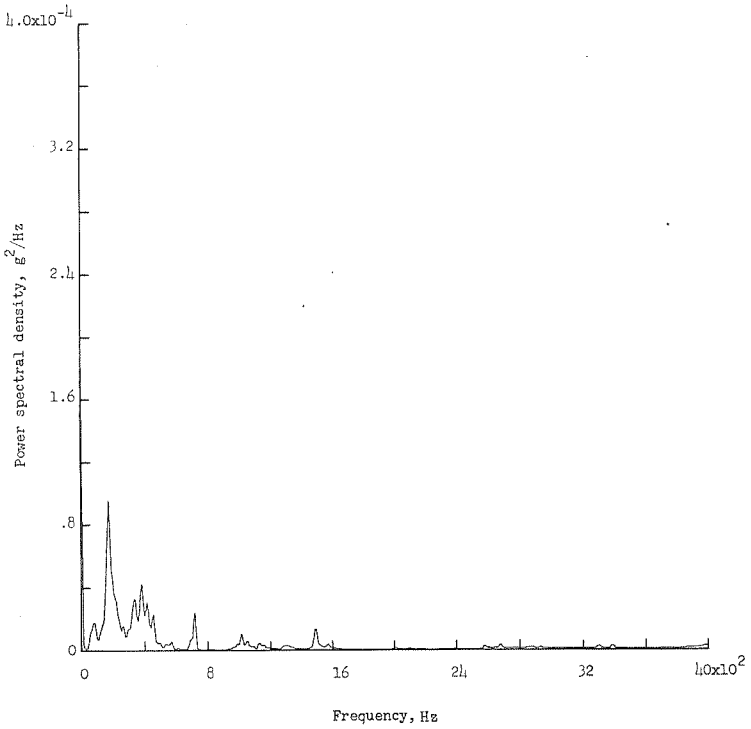

(a) Power spectral density.

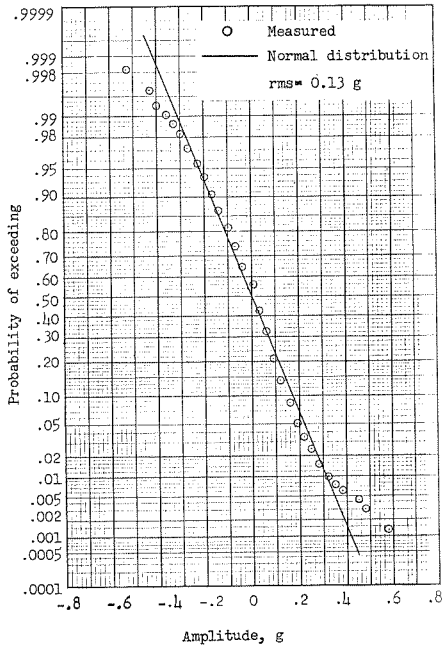

(c) Probability of equaling or exceeding given values of g.

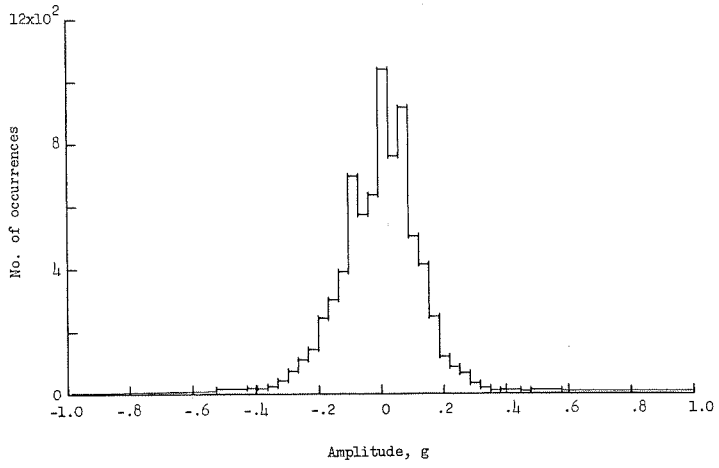

(b) Histogram.

Figure 24.- Lower longitudinal vibration of 1-second sample starting at 5.353 seconds after first-stage ignition.

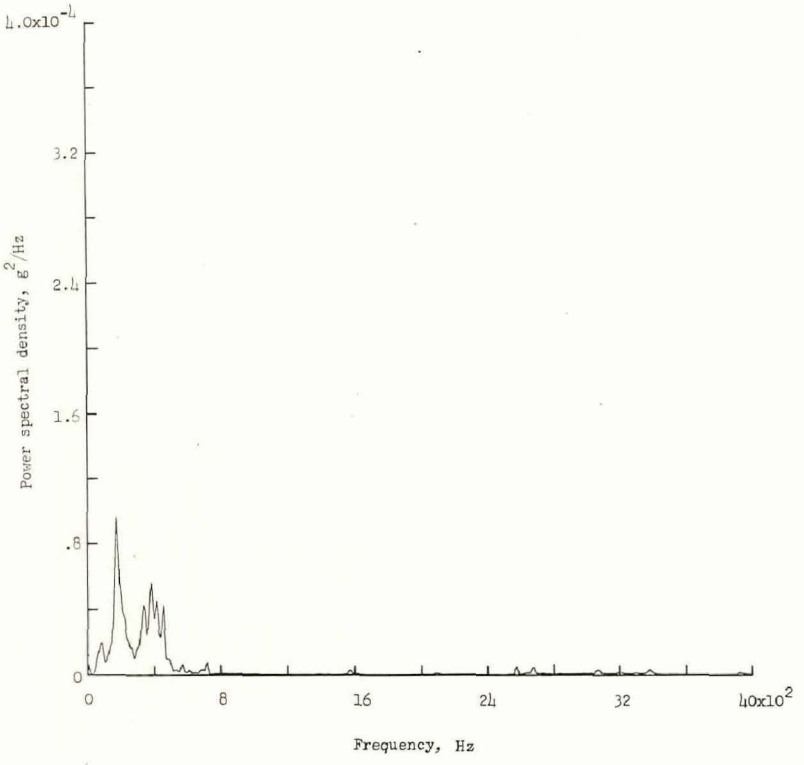

(a) Power spectral density.

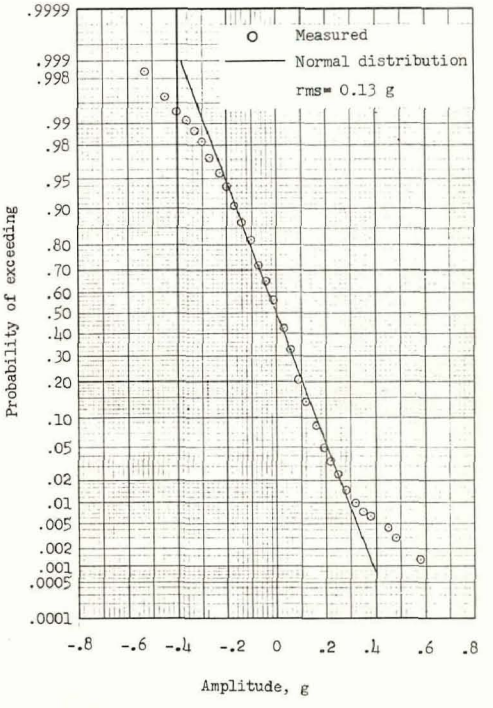

(c) Probability of equaling or exceeding given values of g.

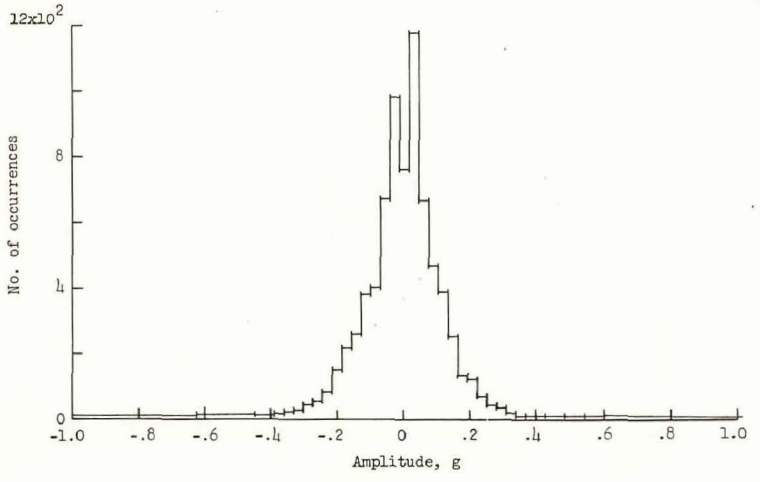

(b) Histogram.

Figure 25.- Upper longitudinal vibration of 1-second sample starting at 5.353 seconds after first-stage ignition.

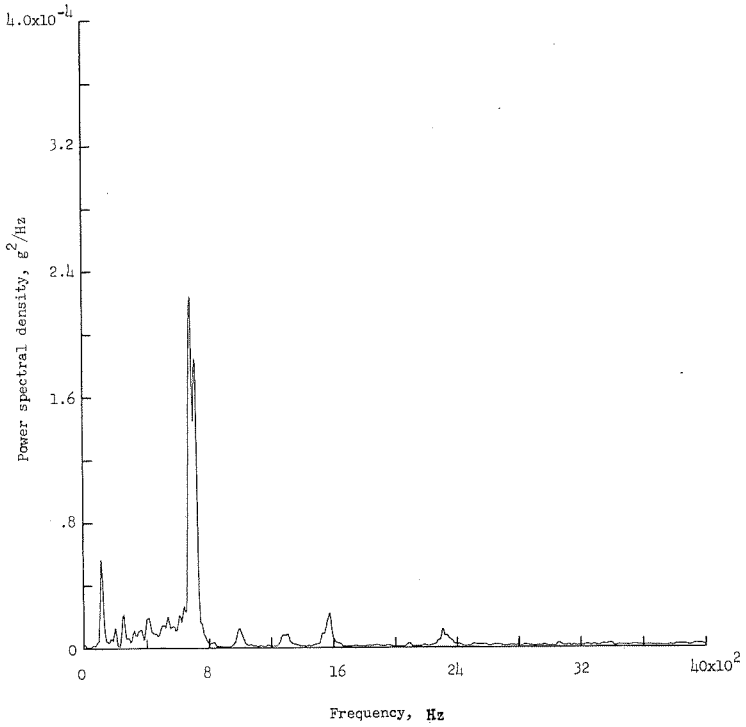

(a) Power spectral density.

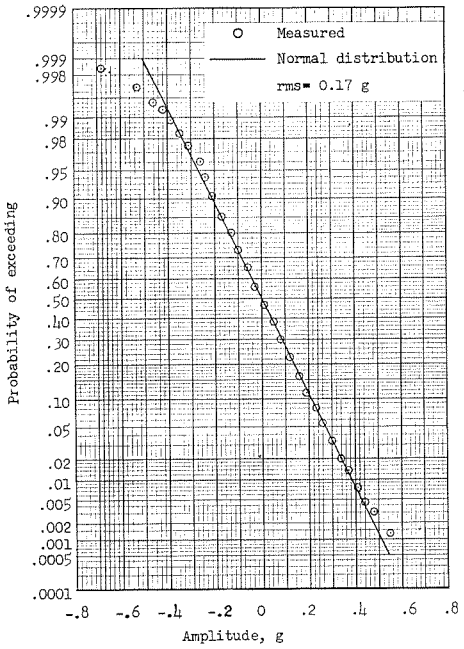

(c) Probability of equaling or exceeding given values of g.

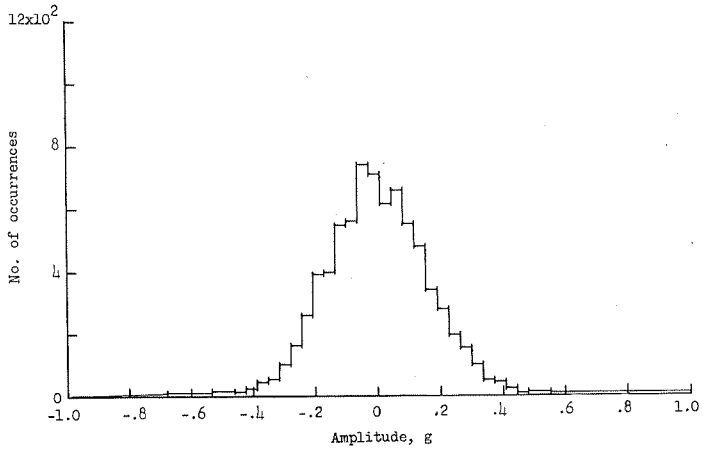

(b) Histogram.

Figure 26.- Normal vibration of 1-second sample starting at 5.353 seconds after first-stage ignition.

"The aeronautical and space activities of the United States shall be conducted so as to contribute . . . to the expansion of human knowledge of phenomena in the atmosphere and space. The Administration shall provide for the widest practicable and appropriate dissemination of information concerning its activities and the results thereof."

—NATIONAL AERONAUTICS AND SPACE ACT OF 1958

NASA SCIENTIFIC AND TECHNICAL PUBLICATIONS

TECHNICAL REPORTS: Scientific and technical information considered important, complete, and a lasting contribution to existing knowledge.

TECHNICAL NOTES: Information less broad in scope but nevertheless of importance as a contribution to existing knowledge.

TECHNICAL MEMORANDUMS: Information receiving limited distribution because of preliminary data, security classification, or other reasons.

CONTRACTOR REPORTS: Scientific and technical information generated under a NASA contract or grant and considered an important contribution to existing knowledge.

TECHNICAL TRANSLATIONS: Information published in a foreign language considered to merit NASA distribution in English.

SPECIAL PUBLICATIONS: Information derived from or of value to NASA activities. Publications include conference proceedings, monographs, data compilations, handbooks, sourcebooks, and special bibliographies.

TECHNOLOGY UTILIZATION PUBLICATIONS: Information on technology used by NASA that may be of particular interest in commercial and other non-aerospace applications. Publications include Tech Briefs, Technology Utilization Reports and Technology Surveys.

Details on the availability of these publications may be obtained from:

SCIENTIFIC AND TECHNICAL INFORMATION OFFICE

NATIONAL AERONAUTICS AND SPACE ADMINISTRATION

Washington, D.C. 20546